Nucleation in Quantum Liquids

Sébastien Balibar

Laboratoire de Physique Statistique de l'Ecole Normale Supérieure
associé aux Universités Paris 6 et 7 et au CNRS
24 Rue Lhomond, 75231 Paris Cedex 05, France

to appear in J. Low Temp . Phys. (dec. 2002)

In order to understand how nucleation proceeds in quantum liquids such as ^4He and ^3He, and the peculiarities of such quantum systems, I present a review of nucleation in condensed matter. By describing successive experiments, I first illustrate the interest and use of the elementary "standard theory" of nucleation. Then I consider its limitations and the existence of "spinodal" and instability limits, possibly in the frame of "density functional" methods. When finally discussing nucleation at low temperature, I consider a further improvement of the standard theory, namely the possibility of nucleation by quantum tunneling. The main emphasis is on crystallization and cavitation in liquid helium, but I also consider water, liquid hydrogen, wetting, the nucleation of steps on crystal surfaces, vortices etc.

PACS: 64.10.+h, 67.20.+k, 67.80.-s

1. INTRODUCTION

Metastable liquids.

For a certain time, a liquid can stay in a metastable state, outside of the stability region in its phase diagram. For example, liquid water can be supercooled down to about -40 °C (233 K).[1] It can also be overheated up to 200 °C under normal atmospheric conditions ($P = 1$ bar). Water has also been stretched to -1400 bar, a remarkably large negative pressure.[2] Such a metastablility is possible because the liquid/solid transition and the liquid/gas transition are discontinuous (*i.e.* "first order") phase transitions. As a result, the interface between a liquid and its vapor has a certain energy per unit area (its surface tension). Similarly, the interface between a solid

and its liquid phase also has a finite surface energy. For a more stable phase (solid or gas) to appear in a less stable one (the metastable liquid), an interface has to be created somehow, and there is an energy cost for that. As a consequence, there is an energy barrier against the nucleation of the stable phase, and metastability is possible.

Nucleation is called "heterogeneous" when it is influenced by the presence of defects, impurities, walls or radiation. This is the most common case in nature. For example, water droplets in clouds freeze around -20 °C, and this temperature depends on the pollution by dust particles and various chemicals. When nucleation is an intrinsic property of the system, it may take place very far from equilibrium conditions and it is called "homogeneous". In this review, I mostly consider homogeneous nucleation, which is simpler to describe quantitatively, and mention briefly heterogeneous nucleation which is more difficult to study since the exact shape or nature of nucleation sites is rarely known.

Negative pressures.

Some people find it difficult to consider negative pressures, although, as we shall see immediately, they are present in everyday life.[3] The pressure of a gas cannot be negative. Suppose that a gas is contained in a chamber closed by a piston. If one pulls the piston, the pressure of the gas vanishes linearly with the density inside according to the equation of state (Fig. 1). Condensed matter is different: liquids and solids have a finite density at zero pressure. Indeed, there exist attractive interatomic or intermolecular interactions which are responsible for the cohesion. Stretching a liquid or a solid means applying a positive stress to it. A negative pressure is nothing but a positive stress.

If our chamber had very clean, smooth and hydrophilic walls, and if it was filled with very pure water instead of a gas, we could pull the piston and reach a moderate negative pressure before vapor bubbles would nucleate. The pressure would follow an extension of the equation of state $P(\rho)$ in a metastable region at negative pressure (Fig. 1). As soon as gas bubbles nucleated, the pressure in the water would rapidly come back to the atmospheric pressure (+1 bar). This is because the gas is highly compressible. Now, surfaces are usually not perfectly clean, and heterogeneous nucleation takes place easily on them. One can see heterogeneous nucleation in a glass of champagne. Some air is first trapped on small defects on the glass surface when it is filled. CO_2 then diffuses towards these few defects where bubbles grow and escape, due to the buoyancy force, at a regular pace. The bottle is free of bubbles because it is much cleaner and smoother inside. This has a great practical importance since, otherwise, if nucleation of bubbles took place in the bottles also, their filling would generate too much foam and

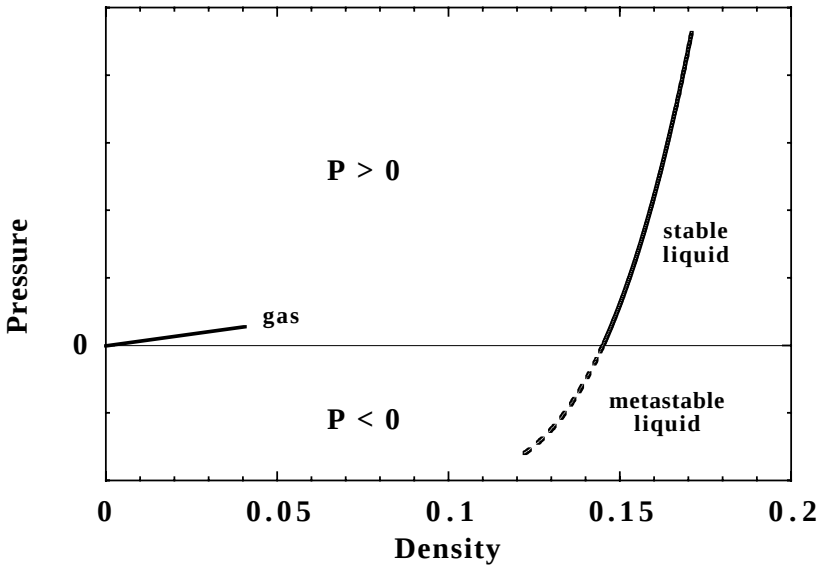

Fig. 1. The pressure of an ideal gas is always positive. For a liquid, the equation of state is such that the pressure can be negative. This is due to the attractive interactions which are responsible for its cohesion, *i.e.* its finite density at zero pressure. The liquid/gas transition being first order, a liquid can be extended in a metastable state along its equation of state.

evaporate too much CO_2 gas.

Negative pressures exist at the top of high trees. Indeed, since the water inside is under hydrostatic equilibrium, its pressure decreases as a function of height. It is lower by 1 bar every 10 meters. If one neglects osmotic pressure effects, and since the pressure at ground level is 1 bar, the pressure at the top of a large redwood tree can be as negative as about -10 bar. Our piston is the 100 meters high column of water pulling down the water at the top. It is maintained there by capillarity. Some authors claim that cavitation can be the factor which, in the end, limits the height of large trees.[4]

The pressure can also be negative in the core of strong vortices.[3] Indeed, according to Bernoulli's law, the quantity $P + \rho v^2/2$ is constant in a non-viscous fluid. Since, in an inviscid vortex, the velocity v is proportional to $1/r$, the inverse radial distance from the core, the pressure can be strongly reduced near this core. A velocity of 45 cm/s is sufficient to create a 1 mbar local depression. If the vortex emerges at the free surface, it makes a local dimple about 1 cm deep. Behind a large, fast rotating propeller, if

the local velocity reaches 15 m/s, the pressure is depressed by 2 bar from the atmospheric pressure and reaches -1 bar. In the ocean, this is enough to trigger cavitation and, when exploding, the bubbles can damage the propeller blade. In superfluid helium, vortices are quantized and the velocity given by $v = \hbar/mr$ (m is the mass of the helium atom). Since there is no viscosity, very large velocities and velocity gradients can occur without dissipation and the vortex core is not limited to a macroscopic value as in normal fluids; it is very small, of order an atomic size. For $r = 2.5$ Å, one finds $v = 60$ m/s and a negative pressure of -2.5 bar.

A historical example is Berthelot's ampoule. In 1850, Berthelot held the world record for negative pressures by cooling down a very clean glass ampoule which he had first filled and sealed with water at high temperature and pressure. When cooled down, the water evolved along an isochore and the pressure decreased. Below a certain temperature depending on initial conditions, the water was under stress. Berthelot reached -50 bar. It is the same method which was used in 1991 by Zheng *et al.*,[2] who reached -1400 bar by making small inclusions of water in quartz crystals which they also filled at very high temperature and pressure, and cooled down afterwards.

Finally, since an acoustic wave is an oscillation in density and pressure, it can induce negative pressures if its amplitude is larger than the static pressure in the medium where it propagates. As we shall see, this has been extensively used for the study of cavitation in fluids.

2. STANDARD NUCLEATION THEORY

2.1. Elementary Theory

2.1.1. The activation energy and the Arrhenius factor

Let us start with the case of cavitation in a liquid, for simplicity. As explained by Landau and Lifshitz,[5] one can model cavitation by calculating the free energy of a spherical vapor bubble inside the metastable liquid (Fig. 2). This bubble is an approximation of the "seed" or "nucleus" which has to appear for the liquid to be replaced by the more stable vapor. This bubble is assumed to have a radius R, and to be filled with a gas at a pressure P_v inside a liquid at pressure P_l. A good approximation of its free energy is

$$F(R) = 4\pi R^2 \gamma - \frac{4}{3}\pi R^3 \Delta G \,, \tag{1}$$

where γ is the surface tension of the macroscopic interface between the liquid and the gas, and ΔG is the difference in Gibbs free energy per unit volume

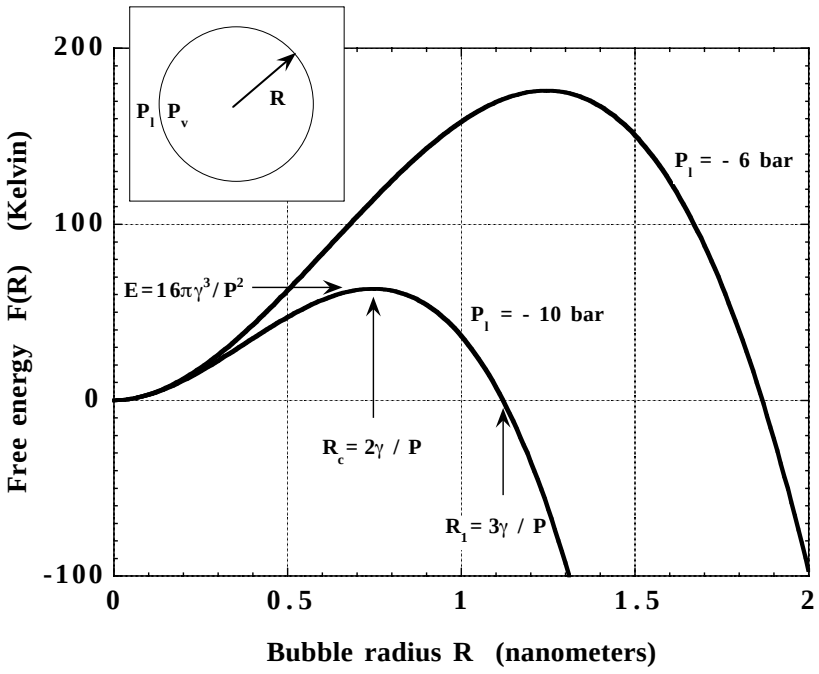

Fig. 2. Within the "standard nucleation theory", one calculates the free energy of a small bubble with radius R as $F(R) = 4\pi R^2\gamma - 4/3\,\pi R^3(P_v - P_l)$. The maximum value of $F(R)$ is the energy barrier against nucleation. It corresponds to the "critical radius" R_c. This graph is drawn according to the values of the surface tension γ of liquid ^{4}He, for two different values of the negative pressure in the liquid.

between the two phases. In the right hand side of Eq. (1), the positive term is a cost in surface free energy, and the second one is a gain in volume energy.

According to Eq. (1), $F(R)$ has a maximum value E for a "critical radius"

$$R_c = \frac{2\gamma}{\Delta G}\ . \tag{2}$$

The maximum is the energy barrier against nucleation, given by

$$E = \frac{16\pi\gamma^3}{3(\Delta G)^2}\ . \tag{3}$$

The main assumption in this simple reasoning is to consider that the surface term is given by the macroscopic surface tension. This is reasonable only

if the critical radius is large compared to the thickness of the interface. It explains why it is often called the "thin wall" or "capillary" approximation. As we shall see below, this result, although rather naive, has proved very useful.

If fluctuations form a nucleus with a radius smaller than R_c, it tends to shrink back to zero size. On the contrary, if the nucleus is larger than R_c, it grows and invades the metastable phase. An important remark by Landau and Lifshitz is that the critical nucleus of radius R_c is under equilibrium with its surrounding phase, even if this equilibrium is unstable. This means that the two chemical potentials are equal and that ΔG can be expressed in terms of the departure $P_l - P_{\rm eq}$ from the equilibrium pressure. Indeed, one usually considers that the temperature inside the bubble is the same as outside. If $\rho_{l,v}$ are the respective densities of the liquid and of the vapor, then one has

$$\Delta G = P_v - P_l = (1 - \rho_v/\rho_l)(P_{\rm eq} - P_l) \ . \tag{4}$$

As one approaches the critical point, the vapor density has to be considered, otherwise it is negligible. In many situations, a good approximation of ΔG is $\Delta G = \mid P_l \mid$. If one considered the nucleation of a solid from a liquid, one would have $\Delta G = (1 - \rho_s/\rho_l)(P_{\rm eq} - P_l)$.

It is also possible to express the departure from equilibrium in terms of the temperature difference from the equilibrium temperature $T_{\rm eq}$. By using the Clausius-Clapeyron relation, one gets:

$$\Delta G = LV(T_{\rm eq} - T)/T_{\rm eq} \ , \tag{5}$$

where V is the molar volume of the stable phase inside the nucleus, and L the latent heat per mole.

Within this "standard theory" one proceeds by writing a nucleation rate per unit volume and per unit time as

$$\Gamma = \Gamma_0 \exp -(E/k_B T) \ . \tag{6}$$

The quantity Γ_0 is called the "prefactor" because it is in front of the Arrhenius exponential factor. It is the product of an "attempt frequency" by a "density of independent sites". Indeed, one counts in how many places (per unit volume) the system can try to pass the energy barrier, and how often it can do it per unit time.

Finally, the probability that nucleation occurs in an experimental volume V during a time τ is an integral of the nucleation rate. One can write it as

$$\Sigma = 1 - \exp\left[-\Gamma_0 V \tau \exp\left(-E/k_B T\right)\right] \ , \tag{7}$$

because it is one minus the probability that nucleation does not occur, which itself decreases exponentially with V and τ. The above equation shows that the nucleation probability varies exponentially as a function of the departure from equilibrium. In a short range of pressure or temperature, it increases from completely negligible to almost equal to one. One can thus define a "nucleation threshold" where the probability Σ is one half. This threshold can be a critical pressure P_c, or a temperature T_c. If E/k_BT is large enough, one can expand the activation energy E around its value $E_c = E(P_c)$, and write:

$$\Sigma = 1 - \exp\left[-\ln 2 \exp\left[-\frac{1}{k_BT}\frac{dE}{dP}(P - P_c)\right]\right] . \tag{8}$$

This expression is more general than the "standard theory" because it does not use any explicit form of the activation energy E. One can then use Eq. (3) to calculate the nucleation line $P_c(T)$:

$$P_c(T) = E^{-1}\left[T \ln\left(\frac{\Gamma_0 V \tau}{\ln 2}\right)\right] . \tag{9}$$

Equation (9) shows that homogeneous nucleation occurs at a pressure (or a temperature) which depends only logarithmically on the prefactor Γ_0, the volume V and of the time τ of the experiment.

2.1.2. Estimations of the "prefactor" Γ_0

Estimating Γ_0 is difficult. It is fortunate that the nucleation threshold depends only logarithmically on it. Some review on this problem is given by D. Oxtoby[6] who explains that a rigorous calculation only exists in the case of the condensation of a supersaturated gas. For this particular case, he develops a kinetic theory for the growth of clusters which includes rates at which atoms (or molecules) aggregate to liquid clusters or evaporate from them. His result is

$$\Gamma_0 = \frac{v_l n^2}{S}\left(\frac{2\gamma}{\pi m}\right)^{1/2} , \tag{10}$$

where v_l is the volume per molecule in the liquid, n is the number density of atoms in the gas, $S = P/P_{\rm eq}$ is a measurement of the supersaturation and m is the mass of atoms. This result resembles the one given by Blander and Katz:

$$\Gamma_0 = N\left(\frac{2\gamma}{\pi m B}\right)^{1/2} , \tag{11}$$

where N is the number density in the metastable phase and B a factor of order 2/3.[7] The term $(\gamma/m)^{1/2}$ might be associated with the frequency of

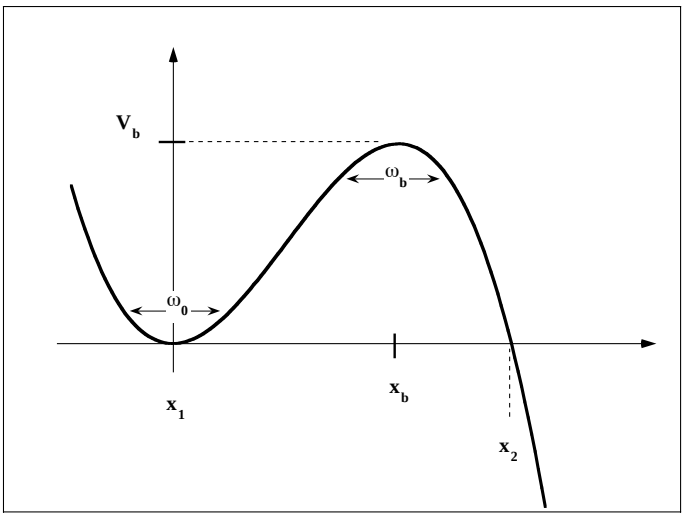

Fig. 3. The Kramers problem of a particle escaping from a potential well V(x). The frequency of oscillations in the well at $x = x_1 = 0$ is ω_0; it would be ω_b in the inverse of the potential at $x = x_b$.

capillary waves at some atomic scale. Indeed, their dispersion relation is

$$\omega^2 = \frac{\gamma}{\rho_l} k^3 \ . \tag{12}$$

If the average distance between atoms in the liquid is a, one has $\rho = m/a^3$ and for a wavevector $k = 1/a$, $\omega = (\gamma/m)^{1/2}$. Except close to the critical point where γ vanishes, the critical nucleus cannot be too large compared to an atomic scale, otherwise its energy is much too large for nucleation to occur at a reasonable rate. As far as I know, no experiment has been precise enough to verify Eqs. (10) or (11).

As also explained by Oxtoby, his kinetic theory cannot be applied to cavitation, since one cannot write rigorous equations for the growth dynamics of bubbles in the dense liquid by using sticking or evaporation probabilities of single atoms. At this stage, it also appears that, on a given site, the system attempts to overcome the energy barrier at a rate which should depend on its viscosity. We imagine that a viscous system takes more time to build a critical nucleus than if it had no viscosity. To include the damping of the dynamics in the calculation of the prefactor is a further difficulty. As far as I know, it has been solved only in the model system of one particle escaping from a one dimensional potential well, the Kramers problem.[8,9] Kramers

considered a particle of mass M in a potential $V(x)$ depending on some variable x (see Fig. 3). Following Grabert *et al.*,[9] we take the particle in the well at $x = 0$, and we consider its possible escape above a barrier of height V_b at $x = x_b$. The frequency of oscillations in the well is

$$\omega_0 = (V''(0)/M)^{1/2} , \tag{13}$$

and they define

$$\omega_b = (-V''(x_b)/M)^{1/2} , \tag{14}$$

They describe the motion in the well by an equation of motion of type:

$$M\frac{d^2x}{dt^2} + \frac{dV}{dx} + M\eta\frac{dx}{dt} = 0 . \tag{15}$$

They define a normalized damping coefficient $\alpha = \eta/2\omega_b$, and they find, for small values of α, the expression

$$\Gamma = \frac{\omega_0}{2\pi}[(1+\alpha^2)^{1/2} - \alpha] \exp\left(-\frac{V_b}{k_B T}\right) \tag{16}$$

for the escape rate. As expected, the damping of oscillations in the potential well decreases the prefactor. One should also notice that it does not change the exponent.

In the general case of a real sample of condensed matter, dissipation is treated in a phenomenological way. Turnbull and Fisher[10] have proposed the expression:

$$\Gamma = \frac{N k_B T}{h} \exp\left(-\frac{\Phi}{k_B T}\right) \exp\left(-\frac{E}{k_B T}\right) , \tag{17}$$

where Φ is an activation energy describing the temperature dependence of diffusion. We notice that they are using a thermal frequency instead of an oscillation frequency in the potential well. Of course it is somewhat surprising to find Planck's constant h in an expression describing a classical process. However, in the frame of Kramers' model, one sees that nucleation cannot reasonably take place if E is too large compared to $k_B T$. Furthermore, except if the potential energy has some kind of pathological variation, the frequency of oscillations in the potential well cannot be extremely different from the height of the barrier V_b/h either. We thus understand that Turnbull's approximation may well work. We also notice that, according to Turnbull's expression, when a liquid is cooled down, the prefactor may be very small if $(\Phi/k_B T)$ is large: instead of nucleation, one observes a glass transition, because the dynamics of the system slows down to nearly zero.

In a system with no dissipation, such as superfluid ^{4}He, Maris[11] proposed that the prefactor is

$$\Gamma_0 = \frac{k_B T}{h} \frac{3}{4\pi R_c^3} , \tag{18}$$

since the attempt frequency is close to a thermal frequency and the density of "independent nucleation sites" is better described by the inverse volume of the critical nucleus than by the number density of atoms. This is another reasonable approximation, the one we used in liquid helium. It might be useful to consider orders of magnitude in this particular example. Cavitation occurs around P_l = -8 bar at 1 K, so that the critical radius R_c is of order 1 nm. A thermal frequency is $kT/h = 2 \times 10^{10}$ Hz at this temperature. The quantity $(\gamma/m)^{1/2}$ is 2×10^{11} Hz. We could also consider the frequency of a sound wave with a wavevector $2R_c$, which is 1.2×10^{11} Hz. Since the inverse volume of the critical nucleus is 2.5×10^{20} cm^{-3}, we conclude that all approximations of the prefactor lead to $10^{31} < \Gamma_0 < 10^{33}$ cm^{-3}s^{-1}. If we now imagine that homogeneous cavitation is studied in a system having a volume V in the range 1 to 10^{-12} cm^3 in a time τ from 1 to 10^{-8} s, we find $V\tau$ in the range 1 to 10^{-20}cm^{3}s. Eventually, since $E/k_BT \approx \ln(\Gamma_0 V\tau)$ for nucleation to occur with a probability of order one, we predict that E/k_BT is in the range 25 to 75 for such a system. It is useful to keep these numbers in mind.

2.2. Supercooling Water and Liquid Hydrogen

I wish now to describe two experiments which illustrate how the standard theory of nucleation can be used. The first one is a study of ice nucleation in supercooled water by Peter Taborek[1] in 1985. At that time, one tried to understand how far liquid water could be supercooled. Water is a complex fluid. H_2O molecules have two covalent O-H bonds, but they also make two H-bonds with neighboring molecules. As a result, the O-atoms tend to be surrounded by 4 H-atoms in the directions of a regular tetrahedron. Water is an "associated liquid", which means that it is made of clusters of tetrahedra which dissociate and re-associate at thermal frequencies (about 10^{12} Hz). Bonding H_2O molecules takes space because of the local symmetry it imposes. This is the origin of well-known anomalies in the physics of water. The first anomaly is, of course, that ice floats on top of water, and this is because, in ice, H-bonds organize H_20 molecules in a hexagonal lattice which is not very dense, while, in water, the smaller number of H-bonds allows the packing of molecules to be denser. The second anomaly has the same physical origin: cold water contracts when warmed

up instead of expanding. The expansion coefficient of water is negative below 4 °C. This is because, as the temperature decreases, more molecules are linked by H-bonds, and that makes the volume increase.

With the idea in mind that water is an anomalous liquid, various authors have predicted further anomalies and instabilities of water, in particular in its metastable region. In 1985, Taborek wanted to see if water could not be supercooled below -40 °C because there was some singularity in the phase diagram there, or simply because this was the typical temperature at which homogeneous nucleation took place.

He designed an experiment in which heterogeneous nucleation had to be suppressed. For this he used very pure water, of course, but he also divided the water in small droplets. This is an important idea. If the water contained a few solid particles which were favorable to the heterogeneous nucleation of ice, they would be isolated in a few contaminated droplets and would not affect the others. Taborek thus made an emulsion of water by mixing it with oil and a surfactant. The oil was "petroleum jelly" and the surfactant either something called STS or STO. By warming up and stirring everything with variable strength, he could obtain a dispersion of droplets with a rather well defined and variable size. When cooling back, the petroleum jelly jammed and the droplets were stable for a long time.

He then measured the rate of nucleation of ice by monitoring the rate at which the latent heat of crystallization was released in his emulsion. For this he put everything in a calorimeter whose temperature was carefully regulated. If heterogeneous nucleation was taking place on the water/oil interface, it would depend on both the nature of the surfactant and the surface area of droplets, that is on their size. He found that the STO surfactant was not good, since he observed a size dependence of the nucleation rate. On the contrary, with STS, the nucleation rate was smaller than with STO, and independent of droplet size. He thus concluded that nucleation was homogeneous with STS (see Fig. 4).

He then tried to compare his nucleation rate with the formula proposed by Turnbull and Fisher [Eq. (17) above]. The activation energy for diffusion Φ made only a small correction, and he found a nice exponential variation of the nucleation rate as a function of T. At that time, the exact value of the energy of the ice/water interface was not known. In fact, he used the standard nucleation theory to determine this interfacial tension, and found that it was 28.3 erg/cm^3 at 236 K. An even better fit was obtained by including a small temperature variation ($d\gamma/dT = 0.1$ erg/cm^{2}K) so that he estimated $\gamma = 31.9$ erg/cm^2 at 273 K. If a singularity existed in the phase diagram of water near -40 °C, it would affect the value of the surface tension. For example, the surface tension would have been strongly reduced as one approached

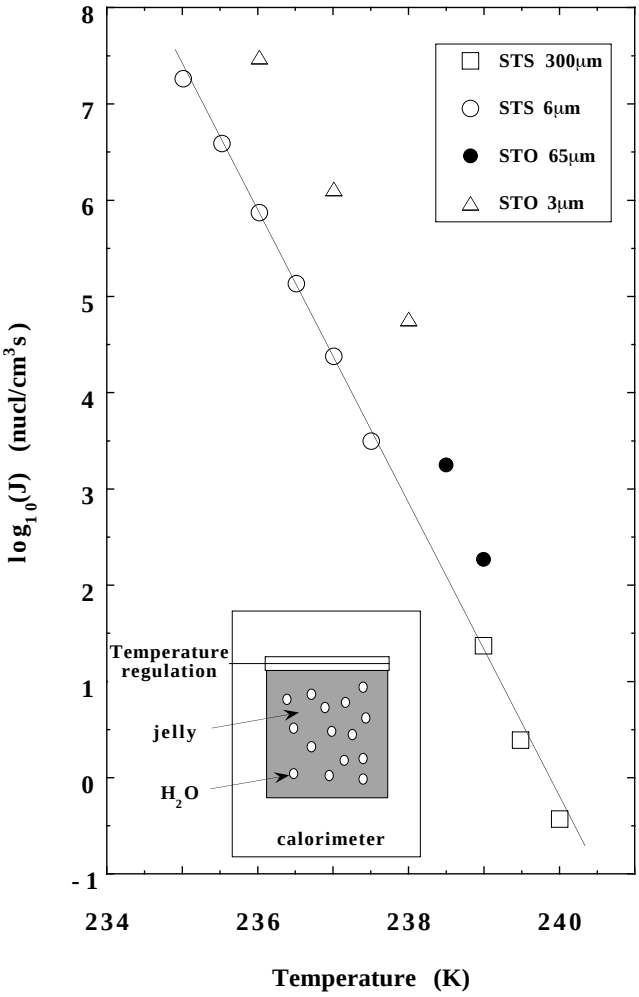

Fig. 4. P. Taborek[1] measured the rate of nucleation of ice in an emulsion of water droplets with petroleum jelly and two different surfactants (STS and STO). In the case of STS, the rate is independent of droplet size, thus independent of the water/oil interface. The nucleation rate depends exponentially on temperature. The standard theory of homogeneous nucleation was used to extract the value of the ice/water interfacial tension.

this singularity. Taborek would not have found such a good agreement with the standard nucleation theory. He thus interpreted his results as evidence that nucleation is homogeneous and that no singularity modifies it around -40 °C. That is why he could use his experiment to determine the surface tension of the ice/water interface.

The experiment by Seidel *et al.*[12] on supercooled liquid H_2 is similar and further illustrates the use of the standard nucleation theory. About at the same time (1986), people were looking for superfluids other than liquid helium, and liquid molecular hydrogen was a possible candidate. H_2 has a triple point in its phase diagram at 13.8 K, so that, contrary to liquid helium, liquid H_2 cannot be in equilibrium down to absolute zero. As had been explained shortly before by Maris,[13] if one could supercool liquid H_2 strongly enough, one could observe its superfluidity around 4 K with many similarities and interesting differences with liquid helium. As in the case of ice, the energy of the liquid/solid interface of H_2 was not known. Maris considered possible values in the range from 0.75 to 1.5 erg/cm^3, and made interesting predictions (see Fig. 5).

As the temperature is reduced below the triple point temperature T_t, the nucleation rate first increases, then passes through a maximum value, and finally decreases sharply (note the logarithmic scale of the vertical axis in Fig. 5). Indeed, the rate is negligible near equilibrium, *i.e.* T_t, because the energy difference ΔG is very small so that the energy barrier E is large. As T tends to zero, ΔG saturates at a finite value, and E/T increases. In between these two limits, Γ has a maximum. Furthermore, the exponential dependence of the nucleation rate on γ is so strong that it reaches values larger than 1 per cm^{3}s if $\gamma = 0.75\,\mathrm{erg/cm^2}$, but it is completely negligible ($\Gamma < 10^{-50}$) if $\gamma = 1.5\,\mathrm{erg/cm^2}$. This behavior is very general: if the surface tension is large enough, one can hope to supercool a system down to absolute zero. Taborek had also predicted a maximum nucleation rate for water at 170 K, but the surface tension is not large enough, and the maximum rate is consequently too large for the supercooling of water to exceed 40 degrees. As shown by Seidel *et al.*,[12] the same happens with liquid H_2.

Seidel *et al.* also divided their liquid H_2 into small droplets. For this they injected it through a small nozzle into pressurized helium gas. The helium was at 15 bar to match its density with that of H_2. More precisely, a temperature gradient was applied to the helium chamber (see Fig. 6), so that the density of helium was decreasing with height. Due to the buoyancy force, liquid droplets floated at a certain height. When they crystallized, they fell down to a different height because solid H_2 is denser, and this made nucleation observable. Seidel and his collaborators could thus count the number of nucleation events as a function of supercooling, and draw a semilog

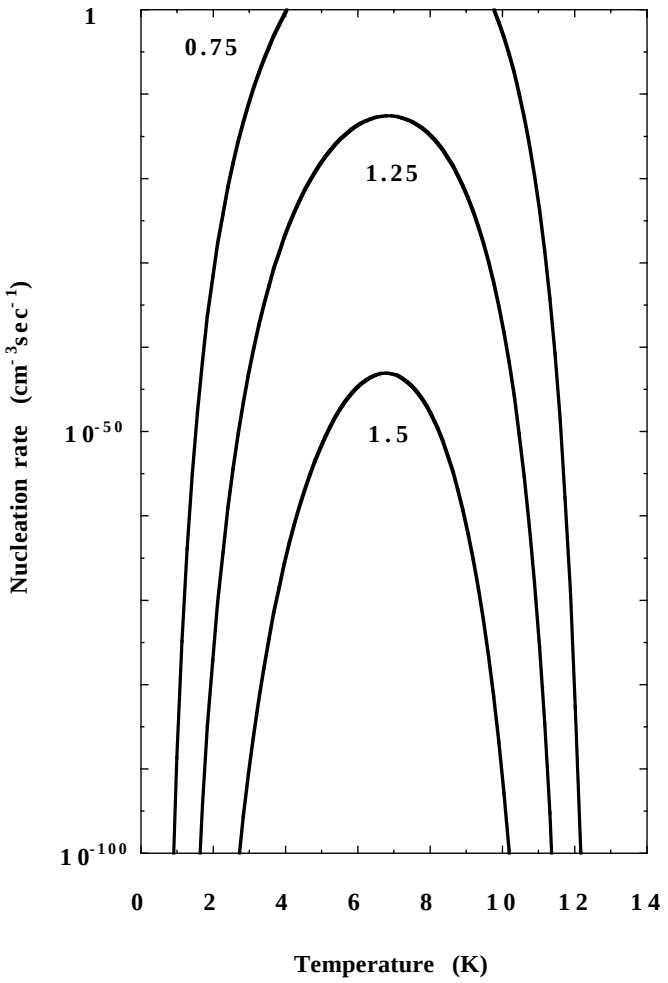

Fig. 5. The nucleation rate of solid H_2 from liquid H_2 as calculated by Maris *et al.*[13] for different values of the solid/liquid interfacial tension (in cgs units).

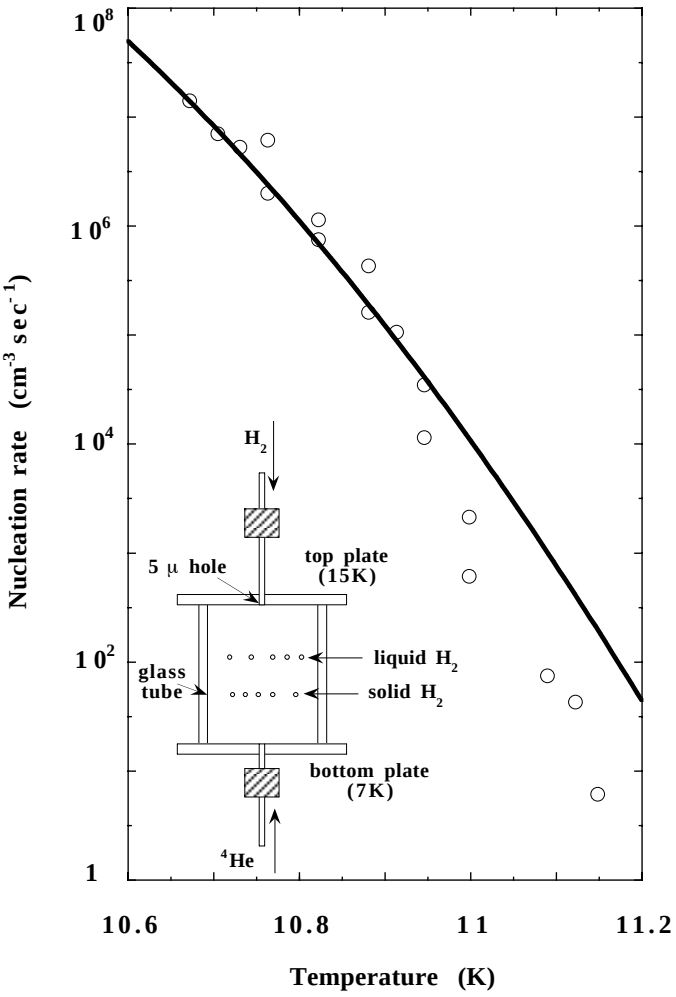

Fig. 6. Seidel *et al.*[12] measured the nucleation rate of solid H_2 from liquid H_2 droplets floating in a pressurized helium vapor. They used the standard nucleation theory to extract the value of the liquid/solid interfacial tension. They used the data at low temperature only because, above about 11 K, convection in the gas perturbs the temperature measurements.

plot of the nucleation rate as a function of temperature as had been done by Taborek. After considering various possible artefacts such as the dissolution of helium in hydrogen, they found a well defined exponential behavior of the rate in a small temperature range around 10.7 K, and used the standard theory to conclude that γ was 0.874 erg/cm^2 at this temperature. This value is not large, and explains why it is not possible to supercool liquid H_2 by more than 20% of its triple point temperature in macroscopic volumes.

Let us finish this Section with two examples where supercooling may possibly be extended down to absolute zero. One concerns superfluid ^{3}He. There are two different phases of superfluid ^{3}He, called A and B. Near the melting pressure at 34 bar, ^{3}He-B is stable below 2 millikelvin, and ^{3}H-A between 2 and 2.5 mK. There is a first order phase transition from A to B. The interfacial tension has been measured by Osheroff *et al.*[14] and found substantial. On the contrary, the difference in free energy ΔG between A and B is not large and saturates to a small value at $T = 0$. If there were no surfaces nor radiations which might both be responsible for its heterogeneous nucleation, ^{3}He-B would never nucleate.[15,16] By using extremely clean experimental conditions, Schiffer *et al.*[17] reached very strong supercooling of ^{3}He-A. It is still somewhat controversial whether suppressing the effect of walls would allow to supercool ^{3}He-A down to absolute zero.

A last example concerns the wetting transition. If a substrate is in contact with a liquid in equilibrium with its vapor, there can be two different situations. Either the liquid spreads ("perfect" or "complete" wetting) or it forms drops which touch the substrate with a non-zero contact angle ("partial" or "incomplete" wetting). Moreover, there can be a transition between partial wetting to complete wetting as the temperature is increased above a critical "wetting temperature" T_w. The wetting transition is a first order phase transition in most cases. If one starts from a high temperature situation where the substrate is covered by a thick layer of liquid, and if one cools the system down, one needs to nucleate dry areas to reach the equilibrium state of this system. Since the line tension of the boundary between dry and wet regions is generally high, and the difference in surface free energies between wet and dry surfaces is not large, it is difficult to nucleate these dry regions.[18] In the case of liquid helium on cesium substrates, it has been shown that the wet situation can be supercooled down to absolute zero. One should notice, however, that, in this particular example, the possible roughness of the substrates favors the wet state and cannot help the nucleation of dry spots.

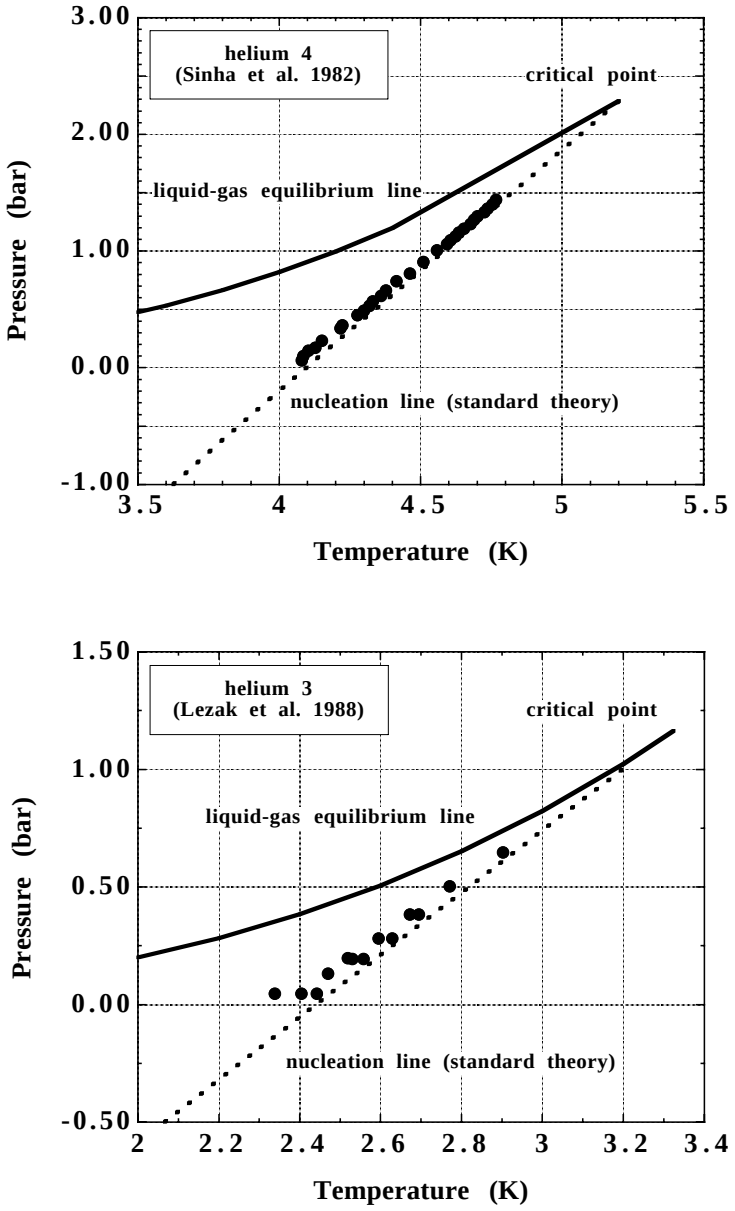

Fig. 7. The homogeneous nucleation pressure of helium gas from overheated liquid helium. Data points are from Sinha *et al.*[19] in the case of ^{4}He, and from Lezak *et al.*[20] in the case of ^{3}He. Agreement is found with the standard nucleation theory (dotted lines, see text).

2.3. Boiling Liquid Helium at High Temperature

High temperature, in this case, means from 4 K to 4.6 K, as was done by Sinha *et al.*[19] in ^{4}He. With this example we start considering cavitation in helium, a model system for the study of nucleation, in my opinion. It also further illustrates the role of wetting and walls. The nucleation of bubbles is usually called boiling when it results from a temperature change, and cavitation when it is from a pressure change, but, in fact, cavitation and boiling belong to the same physics.

Sinha *et al.* used a bismuth crystal which was immersed in liquid ^{4}He. By applying a pulse of current through the Bi crystal, they produced a pulse of heat which warmed up the liquid near the Bi surface. From the magnetoresistance of Bi, they could monitor the local temperature. A careful study as a function of power and pulse width (*i.e.* time), showed that there existed a regime in which bubbles nucleated in the bulk of liquid helium near the surface, not on the Bi surface.

Sinha *et al.* explained that this was due to the very good wetting of Bi by liquid helium. To nucleate a bubble on the surface needed to push the liquid away, and this was apparently more difficult than nucleating a full bubble slightly away from the Bi surface. The temperature at which boiling started was clearly identified as a well defined plateau in the time variation of the Bi temperature. Starting from a given point on the liquid/gas equilibrium curve $P_{\rm eq}(T)$, they could measure precisely the overheating of the liquid and plot a nucleation line in the phase diagram (see Fig. 7). Unfortunately, their method could not be extended below 4 K where the nucleation pressure becomes negative, nor above 4.6 K where the saturated vapor pressure of liquid helium is 1.25 bar, since their glass dewar could not stand a higher pressure. They were not able to measure the nucleation rate.

In order to compare with the standard nucleation theory again, they used the expression proposed by Blander and Katz [Eq. (11)]. They obtained perfect agreement by assuming a product $V\tau = 1$ cm^{3}s and using $\Gamma V\tau = 1$ on the nucleation line. In Fig. 7 (upper graph), I have used the slightly different expression by Maris [Eq. (18)] with a more realistic value $V\tau = 4\ 10^{-5}$ cm^{3}s and the agreement is still good. On the lower graph, the same comparison is shown with the results obtained by Lezak *et al.*[20] in ^{3}He. This work was done with the same method in the same group at Portland State University, a few years later. Once more, the agreement with the standard theory is good. Some more years later in the same group, Nissen *et al.*[21] obtained additional data with a different method which we consider in the next section.

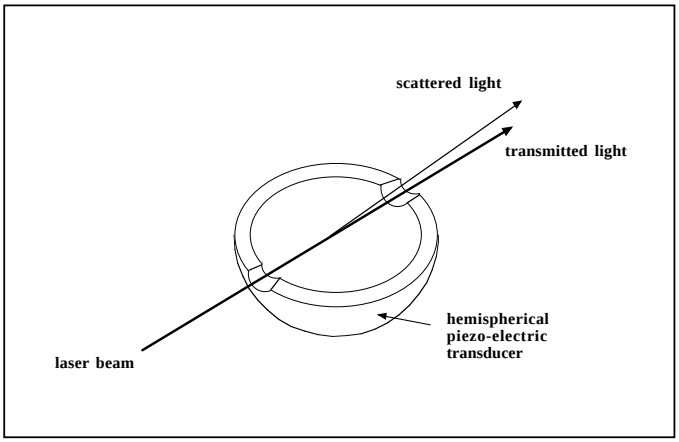

Fig. 8. Nissen *et al.*[21] introduced an acoustic method to study cavitation in liquid helium at negative pressure. A hemispherical piezo-electric transducer generates a sound wave which is focused at its center. The nucleation of bubbles scatters light from a laser beam which illuminates the acoustic focal region.

2.4. The Use of Acoustic Waves for Nucleation Studies

2.4.1. Cavitation in liquid helium at negative pressure

In their pioneering work, Sinha *et al.*[19] noticed that, in order to check the standard theory further, it would be interesting to extend the study inside the negative pressure region. For this purpose, Nissen *et al.*[21] used ultrasound emitted by a hemispherical transducer (Fig. 8). The transducer was a piezo-electric ceramic which was excited by voltage bursts at the frequency of a resonance in a thickness mode. The ac-motion of the inner surface of the transducer emitted a wave in the liquid which was focused at the center by the geometry. At large enough vibration amplitude, the negative swings in the wave produced transient negative pressures. The possible nucleation of bubbles was detected by shining a laser beam through the acoustic focal region: light was scattered by the density modulation in the acoustic wave, it was scattered with a larger intensity at a larger angle by the bubbles when they nucleated.

Nissen *et al.*[21] calibrated the amplitude of the negative swings produced in their experiment by analyzing first the electrical resonance of the transducer (I will come back to this method in Section 2) and also the light scattering from the acoustic wave. They ended up with data points in agreement with both the previous work of Sinha *et al.*[19] and the standard nucleation

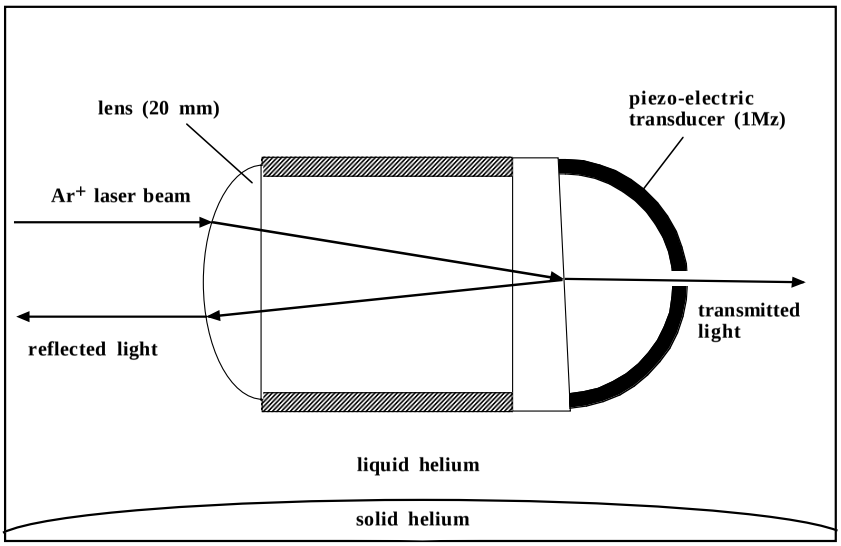

Fig. 9. In order to calibrate the amplitude of their acoustic waves, Chavanne *et al.*[24] introduced a glass plate in their cell. They measured the reflection of light at the glass/helium interface where the hemispherical transducer focuses the acoustic wave. An analysis of the transmitted wave allowed them to study the statistics of nucleation of crystallites at the focus. Since the cell was at the liquid/solid equilibrium pressure, some solid helium was present in the bottom part of the cell.

theory again.

2.4.2. Crystallization of liquid helium

We used the same method at twice their frequency (1MHz instead of 500 kHz) and with significantly shorter bursts (3 to 6 oscillations only in our latest work).[11,22–24] In the experiment by Chavanne *et al.*,[24] we pressed the transducer against a glass plate in order to measure the wave amplitude with some accuracy (Fig. 9). For this we measured the amplitude of the light which was reflected at the glass/helium interface, in the acoustic focal region. Indeed, the reflection coefficient depends on the index of refraction of each medium, which is a function of density. After careful calibration, we extracted the absolute amplitude of the instantaneous density of liquid helium at the acoustic focus, a region of typical size the acoustic wavelength

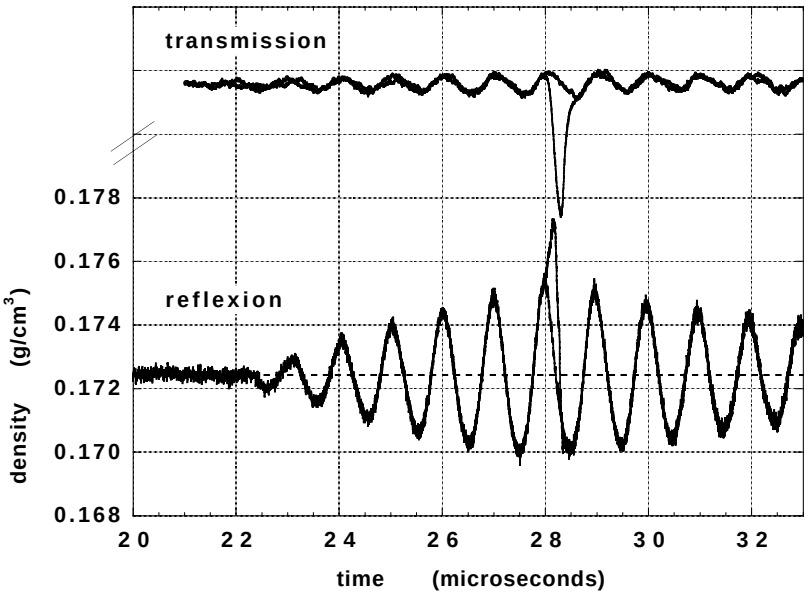

Fig. 10. Some nucleation signals obtained by Chavanne *et al.*[24] in their study of acoustic crystallization. Two pairs of recordings are superimposed on top (transmission) as well as on the bottom (reflection) of this figure. They used sound bursts with a width of 6 cycles. Nucleation of solid helium was observed when the sound amplitude exceeded a threshold density of order 0.003 g/cm^3. The two signals in transmission were recorded with the same excitation level corresponding to this nucleation threshold; the probability of nucleation was 0.45 in this case.

(240 to 360 microns). From the known equation of state of liquid ^{4}He (see Section 2), we could convert densities into pressures. The amplitude of the acoustic pulse shown in Fig. 10 is 0.003 g/cm^3 corresponding to 4.3 bar around a static pressure $P_{\rm stat}$ which is the liquid/solid equilibrium pressure $P_m = 25.3$ bar. We could produce acoustic amplitudes about 5 times larger in liquid helium, despite its low acoustic impedance which makes the coupling of the transducer to the helium weak.

In Fig. 10, two pairs of signals are superimposed. They were obtained during a study of the nucleation of solid helium from overpressurized liquid helium. The lowest pair corresponds to the reflection of light at the glass/helium interface. As explained above, it allows us to measure the instantaneous density of liquid helium in the acoustic wave. Below a certain threshold in amplitude, the signal shape is sinusoidal with an envelope which is governed by the quality factor of the transducer (it is excited during 6 periods and it keeps ringing for some more time after the excitation voltage is switched to zero). This signal is due to the acoustic burst only. Above the threshold, the reflection of light is modified by the nucleation of a crystal near the maximum pressure reached. These two signals are averaged over 1000 pulses.

On top of this graph, the other two superimposed signals are recordings of the light transmitted through the acoustic focal region. They are single shot recordings which were obtained with exactly the same excitation amplitude. One shows light scattering by the acoustic wave only while the other one shows a large negative signal due to additional scattering from the nucleation of a small crystallite. Thanks to the analysis of the transmitted light, it was possible to show that the nucleation was stochastic, and to measure its probability by counting the number of nucleation events divided by the total number of bursts. As shown in Fig. 11 (upper part), Chavanne *et al.*[24] found that the nucleation probability varied continuously from zero to one in a narrow but finite amplitude domain, as one expects from the standard theory. The solid line is a fit of Eq. (9) where the energy E was expanded as a function of density instead of pressure. The asymmetric S-shape of such curves is characteristic of this double exponential formula. It has a rounded foot and a sharper head. One obtains such curves, which are nothing but the integral of events histograms, whenever the prefactor is large enough so that the ratio E/T is significantly larger than one, and a linear expansion of E is thus allowed in the vicinity of the nucleation threshold. Many other experiments have seen such asymmetric S-shape curves in various other contexts as we shall see below.

As also explained by Chavanne *et al.*[24] their fit of the probability curve leads to a measurement of the quantity $dE/d\rho$, the dependence of the activa-

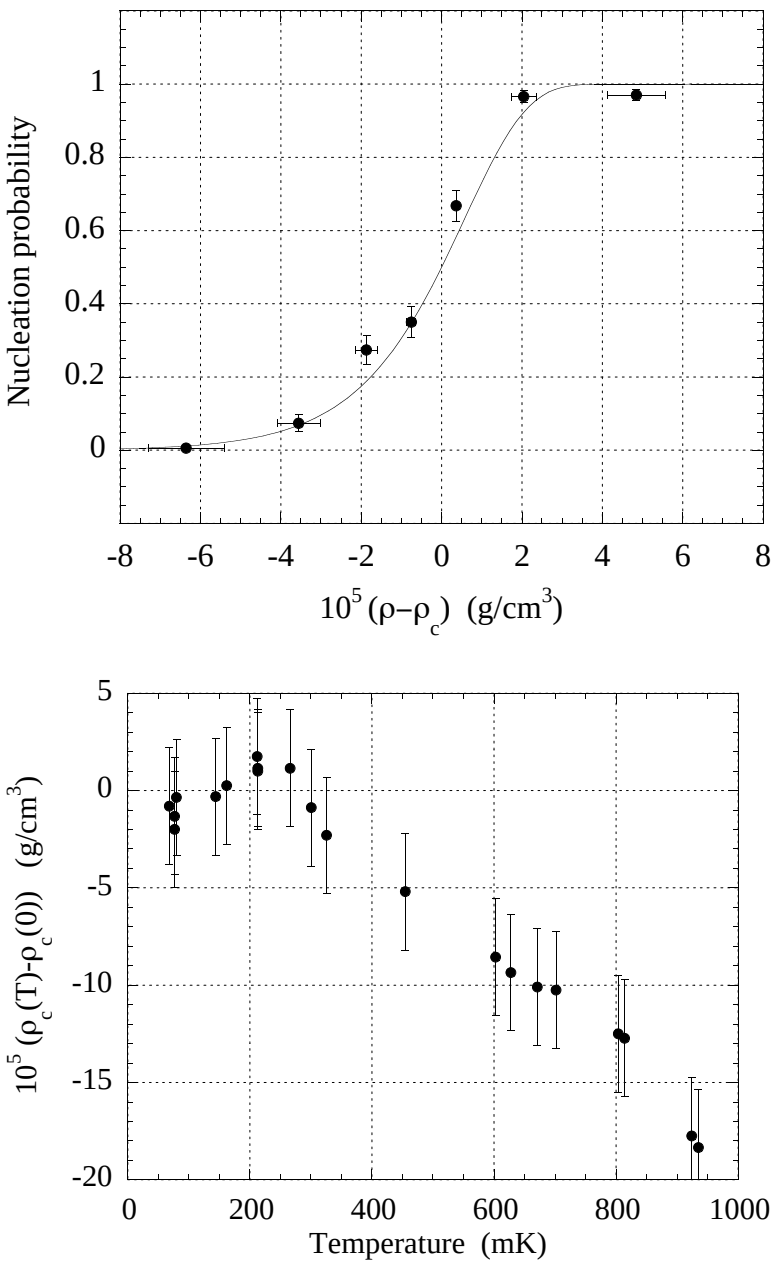

Fig. 11. The nucleation probability (top graph) increases continuously from 0 to 1 in a narrow density interval around ρ_c. The temperature dependence (lower graph) shows a quantum plateau below 300 mK above which it decreases with temperature, as expected for a thermally activated process.[24]

tion energy on the control parameter (here the local instantaneous density). They found $dE/d\rho$ = -3.84 Kcm^3/g. Furthermore, since $\ln \Gamma V \tau$ does not vary much with temperature, one can consider that the ratio E/T is constant along the nucleation line, as a first approximation. Writing $d(E/T)/dT = 0$, one obtains

$$\frac{E}{T} = \frac{dE}{d\rho} \times \frac{d(\rho_c)}{dT} \, , \tag{19}$$

where ρ_c is the threshold density corresponding to a probability 1/2. We thus also studied the temperature dependence of the nucleation line (see Fig. 11, lower part). We obtained $d(\rho_c)/dT$ = -2.6 10^{-4} g/cm^{3}K and finally $E/T = 10$.

I have presented the above description of Chavanne's experiment to show first how the acoustic nucleation technique works, secondly how the analysis of results can distinguish between homogeneous and heterogenous nucleation. If homogeneous nucleation occurred, one could estimate the activation energy from the standard theory. This is because, contrary to previous cases, the liquid/solid interfacial energy is accurately known.[25] E should be of order 3000 K, in obvious contradiction with Chavanne's result. His experiment showed that, thanks to the acoustic technique, it was possible to overpressurize liquid helium by several bars while previous experiments were much more sensitive to impurities or defects and had found only a few mbars.[16] However Chavanne *et al.* demonstrated that his nucleation was still heterogeneous, *i.e.* favored by the glass wall. A further check was to calculate the number of nucleation sites after assuming that the attempt frequency was a thermal frequency $k_B T/h$. He found that it was about one, meaning that one defect was a little more favorable than others to solid helium. If he had observed homogeneous nucleation, this number would have been the ratio of an experimental volume to the critical nucleus volume, a number in the range 10^7 to 10^{11} (depending on whether one considers only the area of the glass/helium interface in the acoustic focal region or its entire volume). This experiment having shown that the optical detection is very sensitive to the nucleation of solid, it opens interesting perspectives in the search of homogeneous nucleation of solid helium, which should occur at much higher overpressures, possibly +200 bar.[24,32]

2.5. Terraces and Steps on Crystal Surfaces

Another interesting example is the nucleation of terraces on crystal surfaces. Below the "roughening transition" crystal surfaces are facetted and the crystal grows by the lateral displacement of steps bounding terraces.[25–27] Usually, the steps are provided by screw dislocations emerging at the crystal

surface, and the growth rate is a quadratic function of the driving force according to the Frank-Read mechanism.[26] It was shown by Wolf *et al.*[27] that, close to the roughening temperature T_R, the dominant growth mechanism is the nucleation of terraces. This new example of nucleation is similar to the one considered above, with two differences.

First it is a two-dimensional process, so that the energy of a terrace with radius R is

$$F(R) = 2\pi R\beta - \pi R^2 a\rho_s \Delta\mu \ , \tag{20}$$

where β is the step free energy per unit length, a is the step height and $\Delta\mu = \mu_l - \mu_s$ is the difference in chemical potential per unit mass between the liquid and the solid. This equation is similar to Eq. (1) and shows that there is a critical radius

$$R_c = \frac{\beta}{a\rho_s \Delta\mu} \ , \tag{21}$$

and an energy barrier

$$E = \frac{\pi\beta^2}{a\rho_s \Delta\mu} \tag{22}$$

for the nucleation of terraces. Wolf *et al.*[27] studied this mechanism with ^{4}He crystals where they had to distinguish three different regimes. At high temperature and driving force, terraces nucleate everywhere at a high rate so that the surface is covered by terraces, this is the "dynamic roughening". At very low temperature, and moderate driving force, the nucleation probability is small and the completion of each layer results from the growth of terraces nucleated one by one. In this case, the growth rate should be simply proportional to $\exp -(E/T)$ with E given by the above equation. In practice, this mechanism is difficult to observe because, at low temperature, it is dominated by the Frank-Read mechanism. However, in the vicinity of T_R, the step energy β vanishes, so that the nucleation of terraces becomes dominant. Its probability being large, terraces nucleate simultaneously at different places and have time to grow on the surface. One thus has to consider their coalescence. There is a characteristic time in this process, which is a/v, the time for the completion of one layer if the growth velocity is v. The density of terraces is the product of this time τ by the nucleation rate Γ, so that the average distance between terraces is $1/(\Gamma\tau)^{1/2}$. Furthermore, in a time τ, the terraces grow by an amount $v_{\rm step}\tau$. Coalescence occurs for

$$v_{\rm step}\tau = 1/(\Gamma\tau)^{1/2} \ , \tag{23}$$

and we find a time τ proportional to the cubic root of the rate Γ. As a consequence, the Arrhenius factor in the growth velocity has to contain $\exp(-E/3T)$ instead of $\exp(-E/T)$.

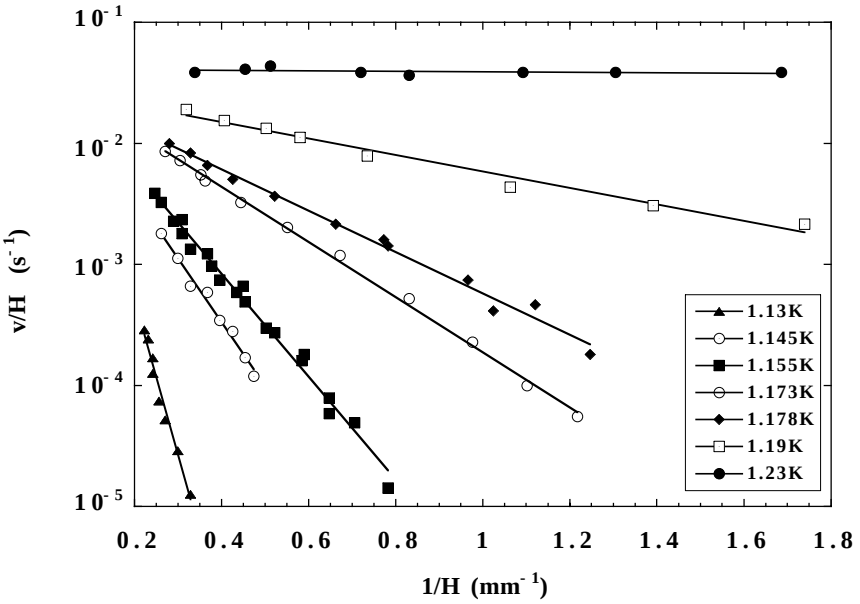

Fig. 12. Wolf *et al.*[25] measured the relaxation of the height of a helium crystal surface. Its velocity v depends on a height difference H which is proportional to the difference in chemical potential between the liquid and the solid (see text). From this semi-log plot, Wolf *et al.* obtained the evidence that the crystal grows thanks to the two-dimensional nucleation of terraces. Each slope is proportional to the square of the step energy which vanishes as the roughening temperature is approached.

Wolf *et al.* studied this by looking at the relaxation to equilibrium of a crystal surface. They could force the existence of a height difference between two parts of a solid-liquid interface in helium. Due to the superfluidity of the liquid, there is no viscosity nor any problem of heat diffusion to slow down the growth process of helium crystals. One can thus watch their relaxation to an equilibrium shape in short times, even when the driving force is as small as a difference in gravitational energy (a height difference). In their experiment, they had $\Delta\mu = (\rho_s - \rho_l)gH$, where H is the height difference driving the relaxation. They compared their measurements of the growth velocity v with the standard nucleation result:

$$v = k\Delta\mu \exp - \left[\frac{\pi\beta^2}{3a\rho_s\Delta\mu k_B T}\right] , \qquad (24)$$

where the prefactor $k\Delta\mu$ was chosen such that when the surface becomes rough due to the proliferation of terraces, the growth rate has to be linearly related to $\Delta\mu$ through a known coefficient k. As shown by Fig. 12, they found very good agreement. In a way similar to what Taborek or Seidel *et al.* did, they used the standard theory to extract the step energy β and its temperature variation, which are crucial quantities in the study of the roughening transition.

2.6. When Does the Standard Theory Work?

The standard theory works when the nucleus is large enough compared to the width of the interface between the stable and the metastable phase. Taborek noticed that, in his case, R_c was about 12 Å, which is larger than the thickness of the ice/water interface, although not much.[1] For cavitation in helium at 4.2 K, R_c is about 40 Å, which is also significantly larger than the width of the liquid/gas interface (less than 10 Å). In the case of Wolf's terraces, R_c is 5000 Å at 1.15 K for a height difference of 2.5 mm, and the step width, which is the correlation length on the facet, is about 1500 Å at this temperature. Wolf *et al.*[25] noticed that at higher temperature ($T > 1.23$ K) their model failed because the width of the steps was larger than the radius R_c as estimated from Eq. (21). Cavitation studies in the close vicinity of the liquid/gas critical point could not be interpreted easily in the frame of the standard theory either, since the width of the liquid-gas interface diverge there. Sinha's experimental data do not extend in this regime. Furthermore, as we shall see below, the standard theory cannot be applied at low temperature either, nor very far from equilibrium.

3. INSTABILITIES AND SPINODAL LIMITS. DENSITY FUNCTIONAL THEORIES

3.1. Cavitation at Low Temperature: the Standard Nucleation Theory Fails

Let us consider the simple case of cavitation again, in the framework of the standard theory. In usual situations, the gas density is negligible, so that $\Delta G = -P_l$ and, according to Eqs. (3 to 9), the cavitation pressure should be

$$P_{\rm cav} = -\left[\frac{16\pi\gamma^3}{3k_BT\ln(\Gamma_0 V\tau)}\right]^{1/2} . \qquad (25)$$

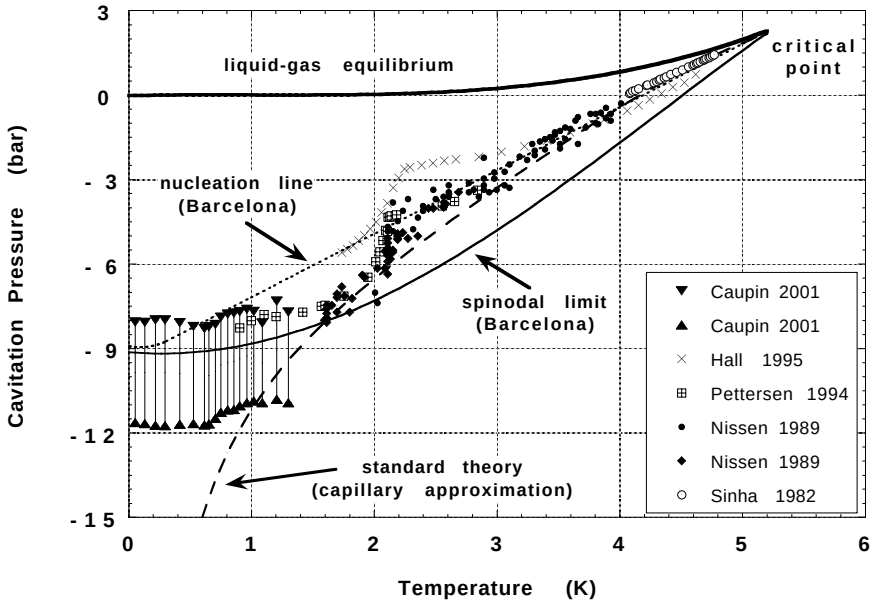

Fig. 13. Summary of cavitation results in ^{4}He.[11,19,21,23,45] Comparison with theory. The experiments by Caupin *et al.*[23] confirm that the cavitation pressure deviates from the predictions of the standard theory at low temperature. Agreement is found with the density functional theory of Guilleumas, Barranco *et al.*[43,44,64] in Barcelona.

This equation predicts a $1/\sqrt{T}$ divergence as T tends to zero, and this does not seem realistic. It is hard to imagine that a liquid can stand an infinite stress. Furthermore, the critical radius $R_c = 2\gamma/\mid P \mid$ is predicted to tend to zero, and this is not realistic either. It is not possible to use macroscopic quantities such as the surface tension γ at an atomic scale. As we shall see now, our cavitation studies in liquid helium have shown that the standard theory fails at low temperature.

We have extended cavitation studies down to 0.04 K by using the acoustic technique described in Section 2.4.[23,22] Instead of finding a divergence of the cavitation pressure at low T, we found a limiting value of about -10 bar. In Fig. 13, the prediction from the standard theory is shown for the product $V\tau = 2.10^{-16}$ cm^{3}s which corresponds to the experiment by Caupin *et al.*[23] Their results are shown as vertical bars between lower bounds and upper

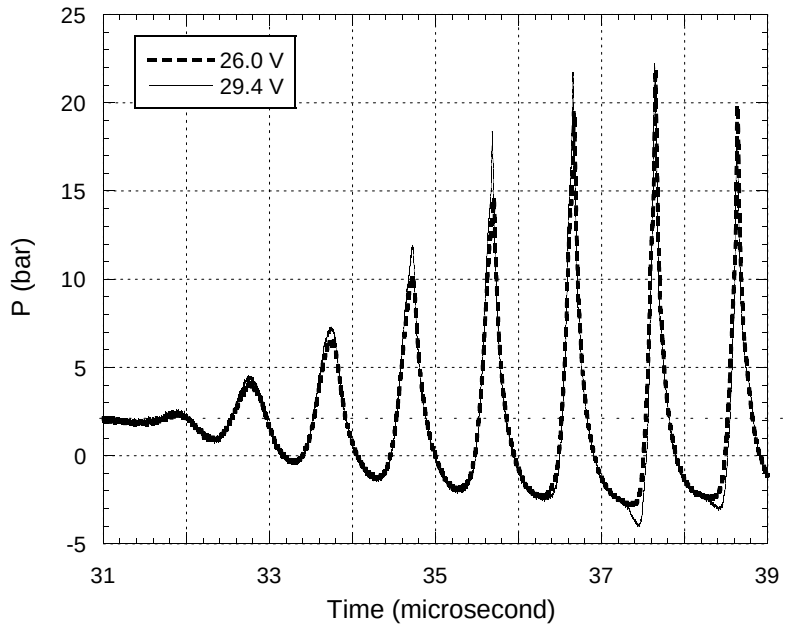

Fig. 14. Chavanne *et al.*[28,29] found strong non-linear effects in the focusing of large amplitude sound waves. The positive excursions of the pressure are sharper and larger than the negative ones. These two signals were recorded with a static pressure of 2 bar at 0.2 K. For an excitation of 29.4 Volt, cavitation is observed at the most negative pressures.

bounds for the cavitation pressure. In this experiment, the hemispherical transducer was used to focus sound into bulk liquid helium, with no glass surface at the acoustic focus, just as in Nissen's original set-up.[21] In the absence of local measurement, it is difficult to know the exact amplitude of the acoustic wave. Nissen *et al.*[21] assumed that non-linear effects are negligible, so that the amplitude of the wave at the center is proportional to the voltage applied to the transducer. This is correct at small amplitude, but it was shown incorrect for the large amplitudes reached in Caupin's experiment. Evidence for the existence of non-linear effects is illustrated by Fig. 14 which shows data taken by Chavanne *et al.*[28,29] at 2 bar. The peak to peak amplitude is about 30 bar and the sinusoidal shape is clearly distorted: the minima are broad and the maxima are sharp, moreover, the shape of the negative swings is not symmetric in time. This is of course because the amplitude is so large that the sound velocity near the minima is much smaller than what it is near the maxima (one half in this case).

Appert *et al.*[28,29] have reproduced such shapes in their numerical calculations of the focusing of large amplitude acoustic waves, and they showed

that the main source of non-linearities is the shape of the equation of state $P(\rho)$, with amplification due to the spherical geometry. Caupin *et al.*[23] have analyzed the dependence of the cavitation threshold as a function of the static pressure. By considering the sign of non-linear effects, they showed that two different kinds of extrapolations respectively lead to an upper bound and to a lower bound for the cavitation pressure in their experiments. A similar calibration method was applied to cavitation in ^{3}He, where they found a limiting cavitation threshold of -3 bar at low temperature (Fig. 15). In ^{3}He also, the standard theory of nucleation was shown to fail. In Fig. 15, the $1/\sqrt{T}$ divergence predicted by the standard theory is shown for two different volumes and times, one corresponding to the experiment by Lezak *et al.* ($V\tau$ = 4×10^{-5} cm^{3}s) and another to Caupin's case ($V\tau = 7\times10^{-15}$ cm^{3}s).[20,23] As can be seen, due to the logarithmic dependence, the nucleation line is only weakly dependent on volume and time, but the divergence at low T is stronger, consequently easier to test, for smaller volumes.

3.2. Spinodal Limits and Equations of State. Density Functional Theories

Just like a solid, a liquid cannot be stretched up to infinite stress without breaking. This is what the existence of a "spinodal limit" means. The existence of such an instability is already present in the van der Waals equation of fluids. This equation writes

$$(P + a\frac{N^2}{V^2})(V - bN) = Nk_BT \ , \tag{26}$$

where a describes an attractive interaction between atoms, and b describes their repulsive hard core a short distance. As we know, this equation describes fluids very well in the vicinity of the liquid/gas critical point ($P_c = a/27b^2$, $k_BT_c = 8a/27b$, $V_c = 3Nb$). After normalizing pressures, temperatures and densities by their respective values at the critical point, the van der Waals equation of state writes:

$$\tilde{P} = 8\tilde{T}\tilde{\rho}/(3 - \tilde{\rho}) - 3\tilde{\rho}^2 \ . \tag{27}$$

Figure 16 shows that this equation of state has one maximum and one minimum which merge together to form an inflexion point at T_c. At the extrema, which are called spinodal points, the derivative $dP/d\rho$ is zero. This means that the compressibility of the fluid is infinite there. If one stretches a liquid so strongly that its density reaches the spinodal point, it cannot resist anymore, it is unstable and has to fall into the gas state. Symmetrically,

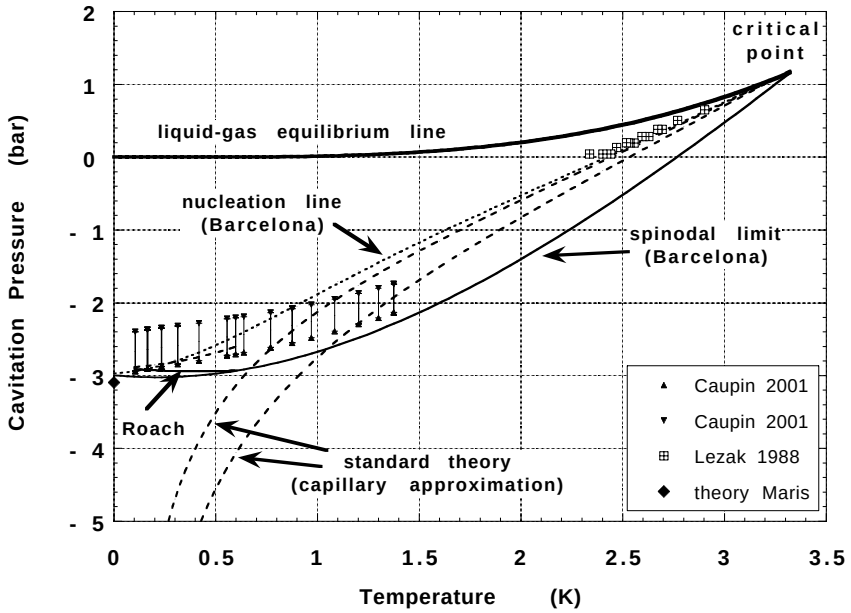

Fig. 15. Summary of cavitation results in ^{3}He.[20,23] Comparison with theories. In ^{3}He as in ^{4}He (Fig. 13), the cavitation pressure is found close to the spinodal limit at low temperature. The nucleation line and the spinodal line labelled "Barcelona" are from the most recent results of Guilleumas, Barranco *et al.*[43,44,64] The two broken lines correspond to the standard theory and two different values of the product $V\tau$, respectively 4×10^{-5} cm^{3}s (upper curve) and 7×10^{-15} cm^{3}s (lower curve). If calculated from an extrapolation of sound velocity measurements by Roach *et al.*,[50] the spinodal line shows a shallow minimum near 0.4 K.

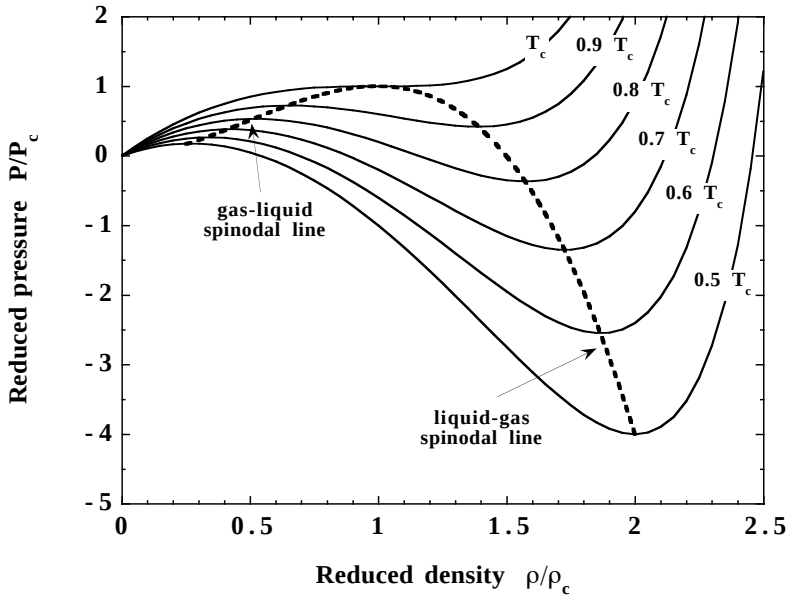

Fig. 16. The van der Waals equation of state describes fluids near their critical point. Different curves correspond to different temperatures. On the spinodal lines, the compressibility is infinite, *i.e.* $dP/d\rho = 0$.

one cannot pressurize a supersaturated vapor above the gas-liquid spinodal limit. The two spinodal points $P_{\rm sp}(T)$ form two "spinodal lines" in the phase diagram. Only one of them is shown in Fig. 19.

The spinodal limit also appears when considering the graph of the energy $E(V)$ of a system with molar volume V. As explained by Maris,[30] E diverges to plus infinity as V tends to zero, it has a minimum for some finite volume and it tends to the reference value $E = 0$ when V tends to infinity (Fig. 17). If one assumes that E is a continuous analytic function of V, then there is an inflexion point in this curve at some value $V_{\rm sp}$. The pressure P being the derivative of E with respect to V, P has a minimum at $V_{\rm sp}$ where it should vary as $(V - V_{\rm sp})^2$. We see that the compressibility is infinite at $V_{\rm sp}$. Since the sound velocity c is the square root of $dP/d\rho$, it should vanish near $P_{\rm sp}$ as $(P - P_{\rm sp})^{1/4}$. Maris[31] modified this argument in 1991, and explained that $E(V)$ is non-analytical in the vicinity of $V_{\rm sp}$ and that c should vary as $(P - P_{\rm sp})^{1/3}$. In fact, he also found a much better agreement of the sound velocity measurement with such a cubic law. As shown in Fig. 18, a plot of c^3 vs P allowed him and later Caupin *et al.*[23] to determine the spinodal pressure at $T = 0$. They found -9.6 bar in ^{4}He and -3.1 bar in ^{3}He.

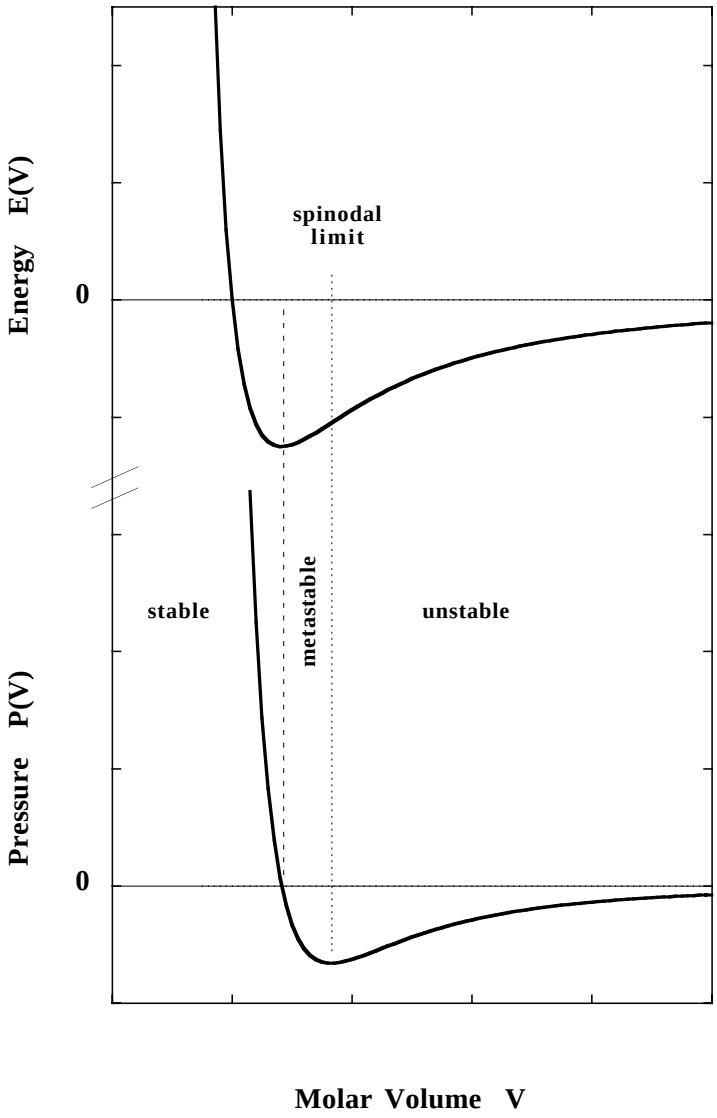

Fig. 17. The energy E and the pressure P of a fluid as a function of its molar volume V. The spinodal limit separates the metastable region from the unstable region.

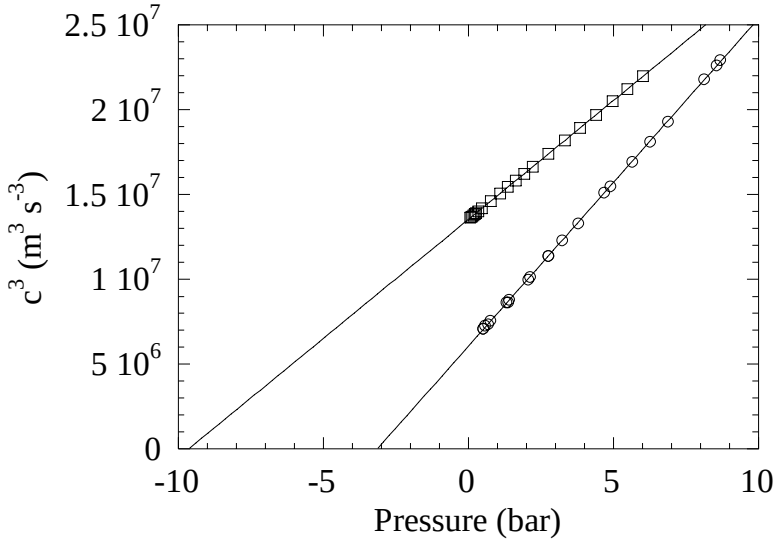

Fig. 18. As explained Maris,[31] the cube of the sound velocity varies linearly with the pressure P. This extrapolation by Caupin *et al.*[23] allows to determine the spinodal limit where the sound velocity vanishes (-9.64 bar in ^{4}He and -3.14 bar in ^{3}He).

According to the latest fit by Caupin *et al.*[23] the equation of state for liquid ^{4}He has the cubic form:

$$P - P_{\rm sp} = \frac{b^2}{27}(\rho - \rho_{\rm sp})^3 \ , \tag{28}$$

with b = 1.4030 10^6 g^{-1}cm^{4}s^{-1}, $P_{\rm sp}$ = -9.6435 bar and $\rho_{\rm sp}$ = 0.094175 g.cm^{-3}.

A similar equation of state was found by at least two other groups using different approaches (see Fig. 19). One is a Monte Carlo calculation by Boronat.[33] The other one, by Dalfovo,[34] uses a "density functional" method which is a fundamental improvement of the standard nucleation theory. It was first introduced in 1959 by Cahn and Hilliard[35] in their historical series of papers. In order to describe a system such as our critical nucleus, where the density is not homogeneous in space, they expanded the energy to first order in powers of the density gradient $\nabla\rho$ and integrated in space:

$$F = \int [f(\rho) + \lambda(\nabla\rho)^2] d^3r \ . \tag{29}$$

In this expression, $f(\rho)$ is the Helmholtz free energy per unit volume for a system with homogeneous density ρ. This is the simplest form of density functional. Without the coefficient λ, the interface between a liquid and its

gas would be infinitely thin. Thanks to the coefficient λ, the energy of the interface γ can be calculated by looking for the particular density profile which minimizes it. The surface tension γ is given by

$$\gamma = \int_0^{\rho_l} \left[\lambda (f(\rho) - \frac{\rho}{\rho_0} f(\rho_0) \right]^{1/2} d\rho \ , \tag{30}$$

where ρ_0 is the liquid density at the equilibrium vapor pressure. This is how λ is adjusted, of course when γ is known.

Maris[36,37] used this simple density functional to calculate the size, density profile and energy of a spherical nucleus at any pressure. Indeed, at -8 bar for example, the standard theory predicts $R_c = 10$ Å, about the same size as the thickness of the liquid/gas interface, so that a more elaborate description is needed. Since the pressure is related to the quantity $f(\rho)$ by

$$P = -f + \rho df/d\rho \ , \tag{31}$$

one can calculate f if one knows the equation of state. It takes into account the existence of the spinodal limit. More elaborate forms of density functionals have been used by Guirao *et al.*[38] who wrote

$$f = f(\rho, T) + \beta \frac{(\nabla \rho)^2}{\rho} + \xi (\nabla \rho)^2 \ , \tag{32}$$

and could reproduce not only the value of the surface tension of liquid helium but also most of the thermodynamic properties as a function of temperature. This allowed them to calculate the whole spinodal line from $T = 0$ to $T = T_c$. As for Dalfovo *et al.*,[34] they included other terms to describe the short range order in the liquid. This allowed them to obtain the whole dispersion relation of phonons in liquid helium as a function of wavevector, which has a famous structure at atomic scale named the "roton minimum" (see Fig. 21).[39]

All the results obtained for the spinodal limit in liquid ^{4}He are summarized in Fig. 19. Not only the calculation by Maris, Boronat *et al.* and Dalfovo *et al.* agree with each other, good agreement is also found with other numerical results obtained in 1996 by Campbell[40] and in 2000 by Bauer.[41,42] As can be seen, the spinodal limit in liquid ^{4}He is rather well established as a line joining the point $P_{\rm sp}(T = 0) = -9.3 \pm 0.4$ bar to the critical point (+2.289 bar at 5.2 K) where there is no difference between the gas and the liquid.

3.3. Comparison with Experiments

Since the compressibility diverges at the spinodal limit, the energy barrier vanishes there: a local density gradient does not cost any energy and

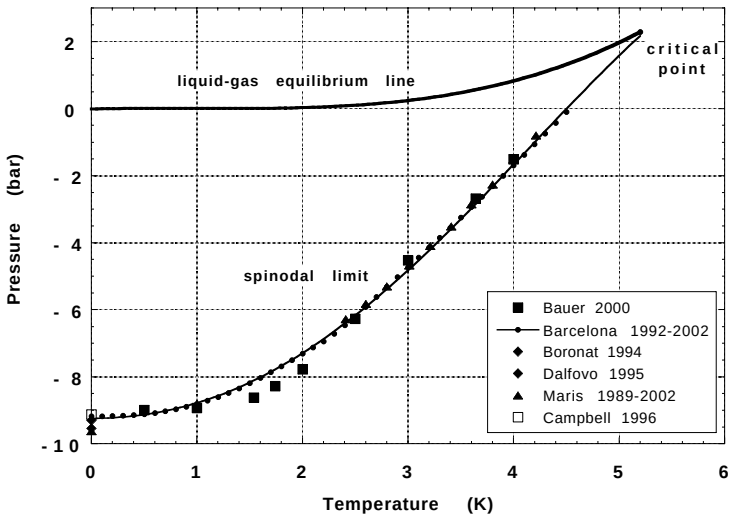

Fig. 19. A comparison between different theoretical predictions of the spinodal limit in liquid ^{4}He. Consistent results are obtained with different methods.

the liquid is unstable. If a system could be quenched down to its spinodal line, its instability would lead to "spinodal decomposition", a scale invariant fractal structure. This is not our case. Indeed, our liquid has a finite size, and it cannot be quenched to negative pressure at infinite speed. Furthermore, this quench cannot be made at strictly zero temperature so that there are thermal fluctuations which allow the system to overcome a finite energy barrier (we will also consider quantum fluctuations in Section 3). As a consequence what is expected and observed is the nucleation of a critical nucleus which has a finite size R_c, not spinodal decomposition. The nucleation is followed by growth which leads to a macroscopic invasion by the stable phase (the gas in the case of cavitation). The existence of the spinodal line is still important to consider in our experimental situation because, in its vicinity, the energy of the nucleus is strongly reduced.

Figures 13 and 15 show nucleation lines which were calculated by using the results of the Barcelona group.[38,43,44] To draw such lines, one needs to know the spinodal line and the activation energy E as a function of pressure and temperature. In the range of activation energies of interest (1 to 100 K

at most), E can usually be well represented by a power law:

$$E = A(T)[P - P_{\rm sp}(T)]^{\alpha} \ , \tag{33}$$

so that the nucleation line is given by

$$P_{\rm cav} = P + \left[\frac{T}{A(T)} \ln\left(\frac{\Gamma_0 V \tau)}{\ln 2}\right)\right]^{1/\alpha} \ . \tag{34}$$

It can be calculated numerically after estimating the prefactor Γ_0 and the product $V\tau$.

Our experiments have confirmed that ^{3}He is about three times more fragile than ^{4}He. Indeed, they confirm that nucleation takes place, in the low temperature limit, near a spinodal pressure which is about -3 bar in ^{3}He and -9 bar in ^{4}He. However, the temperature variation of the experimentally observed cavitation pressure is not very well reproduced by the theoretical predictions. First, the experiments show some kind of cusp in ^{4}He, near the superfluid transition at $T_\lambda = 2.2$ K. We have no clear explanation for this. It might be due to the proliferation of vortices near T_λ which act as nucleation sites for cavitation. The calibration of the negative pressure in the experiments by Pettersen *et al.*[11] is probably not very precise, as well as for Hall *et al.*.[45] In their Monte Carlo simulations Bauer *et al.*[41] have shown that the superfluid transition temperature is nearly independent of pressure, equal to 2.2 K in the metastable pressure region between the equilibrium line and the spinodal line.

At low temperature in ^{4}He, although the magnitude of the cavitation pressure is consistent with predictions, its temperature variation does not seem to agree with them. In Section 3, we will consider this more precisely, since its understanding includes a crossover from the thermally activated nucleation which we have only considered above, to a quantum nucleation below a "crossover" temperature T^*.

In ^{3}He, the magnitude of the cavitation pressure is again in agreement with theory, but its temperature dependence looks too weak. Caupin *et al.*[46] explained this as a consequence of the anomalous sign of the expansion coefficient of ^{3}He at low temperature. As explained in Section 3.4, the role of such an anomaly was first considered in the case of water.

3.4. Maximum Density Lines: the Complex Case of Stretched Water

^{3}He and water have a common anomaly: when sufficiently cold, they contract instead of expanding when heated up. In water, we have seen

that it is a consequence of the H-bonds geometry. In liquid ^{3}He, it is due to its Fermi liquid properties. As recalled by Caupin *et al.*,[46] the thermal expansion coefficient is

$$\alpha_P = \frac{1}{V}\left(\frac{\partial V}{\partial T}\right)_P = -\frac{1}{V}\left(\frac{\partial S}{\partial P}\right)_T \ . \tag{35}$$

As for the entropy of a Fermi liquid, it is given by:

$$S = C_V = \frac{m^*}{m} C_F \ , \tag{36}$$

where m^* is the effective mass of the Fermi quasiparticles and C_F is the heat capacity of an ideal Fermi gas. The variation of S is dominated by the pressure variation of the effective mass m^* which increases with P. As a result, the isobaric expansion coefficient α_P is negative in the degenerate Fermi regime of liquid ^{3}He.

The next interesting point is that the sign of α_P is the same as the sign of the slope of the spinodal line $P_{\rm sp}(T)$ in the phase diagram, as noticed by Debenedetti *et al.*[47] Indeed, it can be shown that the spinodal line is an envelope of isochores, so that its slope is

$$\frac{dP_{\rm sp}}{dT} = \left(\frac{\partial P}{\partial T}\right)_V \ , \tag{37}$$

and

$$\alpha_P = \frac{1}{V}\left(\frac{\partial V}{\partial P}\right)_T \left(\frac{\partial P}{\partial T}\right)_P = \chi_T \frac{dP_{\rm sp}}{dT} \ . \tag{38}$$

If a system has a negative α_P at low T, and a positive α_P above some temperature, then its phase diagram has a line of maximum density (MD) where $\alpha_P = 0$. If this MD line meets the spinodal line, then the spinodal line has a minimum there. On the spinodal line below the minimum, the slope is negative and α_P is -∞, while, above it, it is +∞. This is a remarkable singularity.

In 1982, R.J. Speedy[48] proposed a "stability conjecture", according to which the spinodal limit of water had a minimum at +35°C and -1500 bar, because the MD line of water met it at that point. The MD line of water is known at positive pressure. It goes through the point (4°C, 1 bar), but its extrapolation at large negative pressures is not easy. This is why the shape of the spinodal limit in water is still a matter of debate. In particular, a different phase diagram was proposed later by Sastry *et al.*[49] who argued that the MD line bends back to low temperature at negative pressure and never meets the spinodal, which is consequently monotonic in temperature. Acoustic cavitation studies in water could thus allow a crucial test of the theory of water.

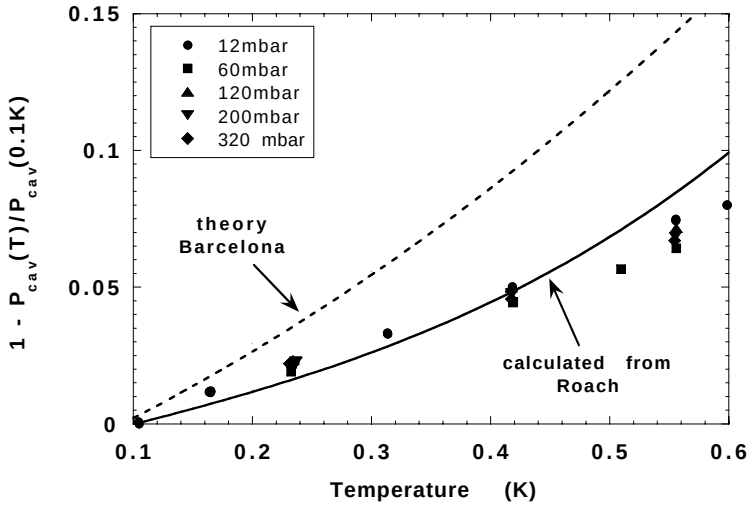

Fig. 20. The temperature dependence of the cavitation threshold in ^{3}He. The best fit is obtained with a spinodal which was calculated by Caupin *et al.*,[46] from sound velocity measurements by P. Roach *et al.*.[50]

Let us come back to ^{3}He. Caupin *et al.*[46] also noticed that an extrapolation of sound velocity measurements by Roach *et al.*[50] led to a shallow minimum in the spinodal line around 0.4 K. The link with the sign of the expansion coefficient was not only supported by theoretical considerations but also by measurements of the expansion coefficient by Boghosian *et al.*[51] Finally, the existence of this minimum slightly modified the temperature dependence of the cavitation line in liquid ^{3}He. As shown on Fig. 20, it is still monotomic but with a smaller slope than predicted by the Barcelona group who used a monotonic spinodal line in their calculation.

3.5. Other Possible Instabilities

The spinodal limit is a line in the phase diagram where the system is unstable. Its compressibility being infinite, its response to a macroscopic stress is infinite. This phenomenon can be generalized. In the case of the liquid/solid transition, no experiment has ever shown the existence of a similar instability. It is not even obvious that it exists. However, the case of helium is again interesting for the following reason. The dispersion relation of elementary excitations in superfluid ^{4}He is known to show a "roton" branch

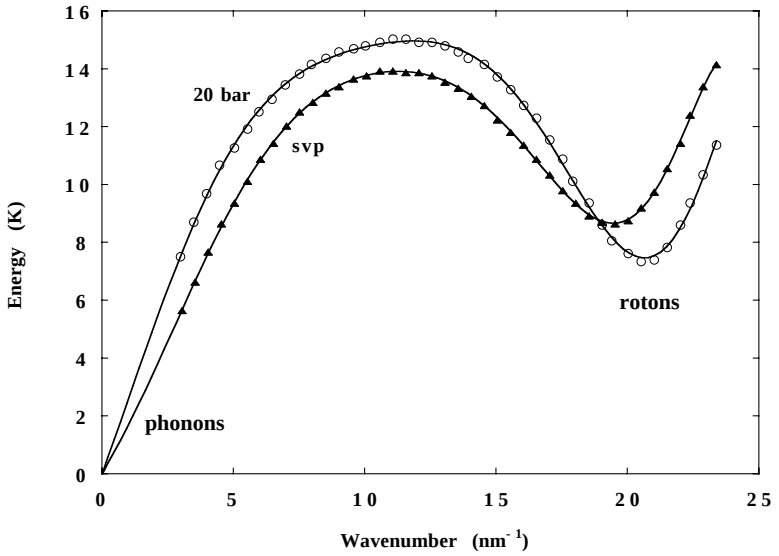

Fig. 21. The phonon-roton spectrum of superfluid ^{4}He. The data points are taken from the neutron scattering experiments of Gibbs *et al.*[52] at 0.5 K. The solid lines are guides to the eye.

first proposed by Landau in 1941 (Fig. 21). Originally, Landau thought that rotons were kinds of quantized elementary vortices. In fact, it is now generally accepted that rotons are particular phonons. Their wavevector is so short that they can be considered as single particles dressed by the interactions of their neighbors.[41] It has been shown experimentally that the minimum energy of rotons (their "energy gap" Δ) decreases with pressure. This behavior is reproduced by the density functional theory of Dalfovo.[34] It seems that, as the density increases, the short range order around each ^{4}He atom increases, and the phonon-roton spectrum resembles more and more the phonon spectrum of a crystal in extended zone representation.

According to recent calculations using Dalfovo's functional, the roton energy should vanish around +200 bar.[32] Supposing that one could overpressurize liquid helium up to such a high pressure, what should happen? This is reminiscent of another instability which concern the free surface of liquids when charged. As shown by Leiderer,[53] it is possible to charge the free surface of superfluid helium. Electrons float on top of the liquid and their density can be varied by applying a variable voltage across the surface. The presence of charges modifies the dispersion relation of surface waves. At large electron densities, this relation acquires a minimum at a wavevector which is the inverse capillary length. If the voltage is further increased, the minimum

goes to zero. A soft surface mode has appeared and a "dimple instability" develops. This means that a corrugation spontaneously forms, and the free liquid surface changes into a regular array of dimples. Could a similar phenomenon occur in liquid helium at +200 bar? Why not? The wavevector of the roton minimum is 2π over the average distance between neighbors (3 Å) and this possible instability would probably trigger the appearance of the crystalline state. This was first proposed in 1971 by Schneider and Enz.[54] A soft roton mode corresponding to a divergence of the response function at finite wavevector (instead of zero wavevector for the usual case of the liquid/gas transition), I do not see why one could not call this instability a "liquid/solid spinodal line". Its study is in progress in our laboratory.

There are more common instabilities which play a role in nucleation. When a non-wetting fluid is pushed through a hole, it makes first a small meniscus with a small curvature. As the pushing pressure increases, the curvature increases. When the meniscus reaches a hemispherical shape, its curvature radius has its minimum possible value and it becomes unstable, the liquid pops through the hole. This is a generic example of a system in a cubic potential well $V(x)$ which depends on some parameter λ. The instability occurs at a critical value λ_c where the potential barrier becomes an inflexion point. One can show that the energy barrier varies as the 3/2 power of $(\lambda - \lambda_c)$. There are several examples of this behavior. One is the heterogeneous nucleation of solid helium on defects. As shown by Ruutu *et al.*,[55] the threshold pressure at which helium crystals appeared in their experiment was drastically reduced by the presence of favorable defects on the walls of their cell.[16] They modelled the observed activation energy as a function of pressure by such a 3/2 power law. I believe that this 3/2 power dependence is present in many examples of heterogeneous nucleation where the barrier does not correspond to the creation of an interface but to the escape of an already existing interface from a favorable site.

Another example is the nucleation of vortices in a superfluid flow through a hole. Vortex rings are nucleated as soon as the flow velocity exceeds a critical value v_c. According to Varoquaux *et al.*,[56] this occurs in the fluid near a wall defect which locally induces a maximum velocity. The energy of a vortex ring depends on its size and on the velocity of the fluid around. It vanishes at the critical velocity. As well as several other groups, they have observed the stochastic nature of the nucleation of vortices and its temperature dependence. In their model, the energy barrier for vortex nucleation has the same 3/2 power dependence on $(v - v_c)$. A last, similar example is that of the Josephson junction in superconductors. A weak link between two superconductors can pass a current with zero voltage up to a certain value I_c. Above I_c, the voltage across the junction is finite. Devoret *et al.*[57] have

performed an extensive study of how the junction jumps from a zero voltage state to a finite voltage state. Their model uses again a $(I - I_c)^{3/2}$ dependence of an energy barrier, and they have found excellent agreement with a linear dependence of the 2/3 power of the logarithm of their nucleation rate as a function of the current I through the junction.

4. QUANTUM NUCLEATION

4.1. The Main Theoretical Ideas and Predictions

In order to pass an energy barrier, a system does not necessarily have to use thermal fluctuations and go over it, it may tunnel through it by a quantum mechanism. Since thermal fluctuations vanish in the $T = 0$ limit, one expects the quantum mechanism to be dominant below a certain "crossover temperature". This is a further improvement which has to be made to the standard theory of nucleation. I wish to describe first the predictions in the case of the one dimensional particle, and then explain how calculations have been made in the more difficult case of a condensed matter sample.

Let us again consider a one-dimensional potential well (Fig. 3) and a particle of mass M inside it. As explained in Landau and Lifshitz,[58] the tunneling rate can be expressed as

$$\Gamma_Q = \Gamma_{Q0} \exp\left(-\frac{B}{\hbar}\right) , \tag{39}$$

where B is an action which can be calculated in the WKB approximation. It is expressed as

$$B = 2\int_{x_1}^{x_2} \sqrt{2MV(x)}dx \ . \tag{40}$$

The particle is supposed to enter the barrier with zero kinetic energy at x_1 and to leave it with the same zero energy at x_2. An alternative expression is obtained when one knows the time evolution which minimizes the action. It writes

$$B = 2\int_{t_1}^{t_2} \left[\frac{1}{2}Mv^2 + V(x(t))\right] dt \ , \tag{41}$$

where the sum of the kinetic energy and of the potential energy appears. As noticed by Maris,[37] Eq. (41) illustrates the fact that the rate at which the particle wavefunction is attenuated as a function of time is the amount by which its energy is not conserved. The time for the particle to tunnel through the barrier is $\tau_t = t_2 - t_1$. The difficult problem, of course, is to calculate B. Even more difficult is the calculation of the prefactor Γ_{Q0}.

This problem has a long history marked by the names of Langer,[59] Lifshitz and Kagan,[59,60] Coleman,[59–61] Caldeira and Leggett,[62] among others. In order to include the effect of dissipation in Kramers' problem, Grabert *et al.*[9] used the "functional integral approach" introduced by Caldeira and Leggett. He calculated the classical escape rate, the quantum escape rate and the crossover from one to the other. As we saw in Section 1.1.2, he found that, in the classical regime at high temperature, the escape rate is

$$\Gamma = \frac{\omega_0}{2\pi}\left[(1+\alpha^2)^{1/2} - \alpha\right] \exp\left(-\frac{V_b}{k_B T}\right) , \tag{42}$$

where ω_0 is the frequency of oscillations in the well, V_b is the potential barrier, and the dimensionless coefficient $\alpha = \eta/2\omega_b$ describes the damping of the motion in the well. We had noticed above that, in this classical limit, dissipation reduces the prefactor but does not affect the Arrhenius exponent. The situation is the opposite in the quantum limit. When T tends to zero, for weak damping and in the simpler case of a cubic potential where $\omega_0 = \omega_b$, Caldeira and Leggett predicted a quantum rate which was reproduced by Grabert as

$$\Gamma = \frac{12}{\sqrt{6\pi}}\frac{\omega_0}{2\pi}\sqrt{\frac{V_b}{\hbar\omega_0}} \exp\left[-\frac{36}{5}\frac{V_b}{\hbar\omega_0}(1 + \frac{45\zeta(3)}{\pi^3}\alpha + ...)\right] , \tag{43}$$

where the Rieman function $\zeta(3)$=1.202. As one sees, it is now the action which depends on dissipation, not the quantum prefactor. We also see that the action B is about $2\pi V_b/\hbar\omega_0$ and that dissipation increases it, so that it reduces the quantum tunnelling probability. On the contrary, the quantum prefactor is independent of dissipation.

Finally, Grabert also gives an expression for the crossover temperature:

$$k_B T^* = \frac{\hbar\omega_b}{2\pi}\left[(1+\alpha^2)^{1/2} - \alpha\right] , \tag{44}$$

which shows that it is determined by the curvature of the potential at the top of the barrier, and that dissipation reduces it. The quantity $2\pi/\omega_0$ is the typical tunnelling time τ_t. These predictions have been accurately compared with the properties of superconducting Josephson junctions.[57] Very good agreement was found for the effect of dissipation which could be varied with a resistor in parallel with the junction. A similar comparison is in progress for the nucleation of vortices in superfluid junctions.[56]

4.2. Quantum Cavitation in the Thin Wall Approximation and in a Continuous Medium

The problem of cavitation is more difficult to calculate. The physics involved may be easier to appreciate if we start with the thin wall approximation. It has been calculated first by Lifshitz and Kagan,[60] then revisited by Maris.[37] In this approximation (Fig. 2), the bubble enters the barrier at $R = 0$ where the energy is zero, and it leaves the barrier at $R_1 = 3\gamma/ \mid P \mid$ where the energy is also zero (see Fig. 2). A calculation of the kinetic energy K of the fluid makes it possible to obtain the effective mass M of the moving bubble. As it expands, it pushes the liquid away. This creates a radial velocity field which is easy to calculate since it is assumed that there is no viscosity. The total kinetic energy is the integral of $\rho v^2/2$, given by the expression:

$$K = 2\pi\rho R^3\dot{R}^2 = 1/2M\dot{R}^2 \ , \tag{45}$$

so that the mass is

$$M(R) = 4\pi\rho R^3 \ . \tag{46}$$

We see that the mass depends on the variable R, and consequently varies during the tunnelling process. The action B is then calculated as

$$\begin{aligned} B &= 2\int_0^{R_1}\sqrt{2M(R)V(R)}dR \\ &= 2\int_0^{R_1}\left(32\pi^2\rho\gamma R^5(1-R/R_1)\right)^{1/2}dR \\ &= \frac{135\sqrt{6}\pi^2\gamma^4\rho^{1/2}}{16 \mid P \mid^{7/2}} \ . \end{aligned} \tag{47}$$

We see that the action B has a pressure dependence which is slightly different from the energy barrier E, which was proportional to $1/ \mid P \mid^2$.

Nakamura *et al.*[63] argued that, due to the zero mass in the initial state which is a bubble with zero radius, this calculation by Lifshitz and Kagan was wrong by many orders of magnitude. They considered that the bubble had a zero point energy which was large, since the mass was zero. According to them, the tunnelling should take place from some energy level intermediate between zero and the top of the barrier. I believe that this is an artefact of their thin wall approximation, and that it is not physical. The initial state is homogeneous, it is not a narrow hole in the liquid, such as a bubble with zero radius. Since quantum nucleation occurs close to the spinodal limit, density functional calculations show that the initial state is a wide shallow depression in density, not a narrow deep hole. This is a very different configuration which we now have to examine.

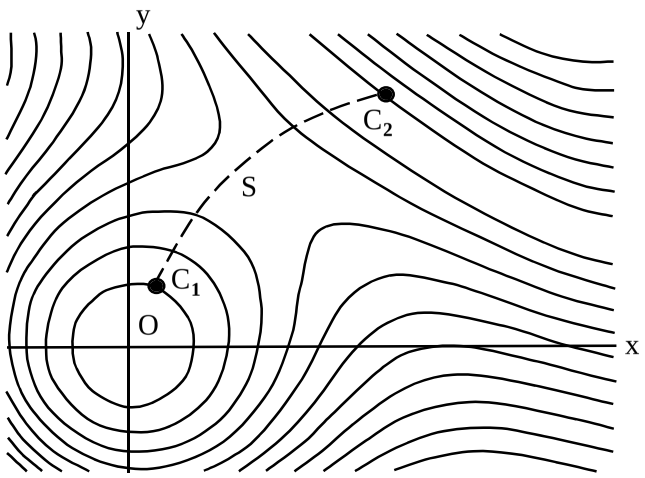

Fig. 22. The energy of liquid helium depends on the configuration of its density field, which Maris[37] represents here in two dimensions for simplicity. Quantum tunnelling occurs through an energy barrier from a configuration C_1 to a configuration C_2 which has the same energy.

Maris[37] extended the work of Lifshitz and Kagan by using the interesting results of Coleman. The tunnelling has to be considered in the space of configurations which has much more than one dimension. The initial state is a homogeneous configuration at negative pressure, consequently a density which is reduced with respect to the equilibrium density at $P = 0$. The final state is a hole, more precisely a density configuration which is inhomogeneous, which can be assumed to have spherical symmetry, but which is not known. Not known either is the trajectory in configuration space which continuously links the initial state to the final state. This trajectory has to be optimized in order to minimize the action. If one reduces the configuration space to two dimensions only (consider, for example, some size of the bubble and some width or depth of its density profile), one can draw a landscape with equal energy lines in it (Fig. 22). Our problem is to find an optimal trajectory from a set of initial configurations (the line C_1) to a set of final configurations (the line C_2).

Coleman[61] demonstrated a very important property of this optimal trajectory. Suppose that one inverts the potential, which means that one re-

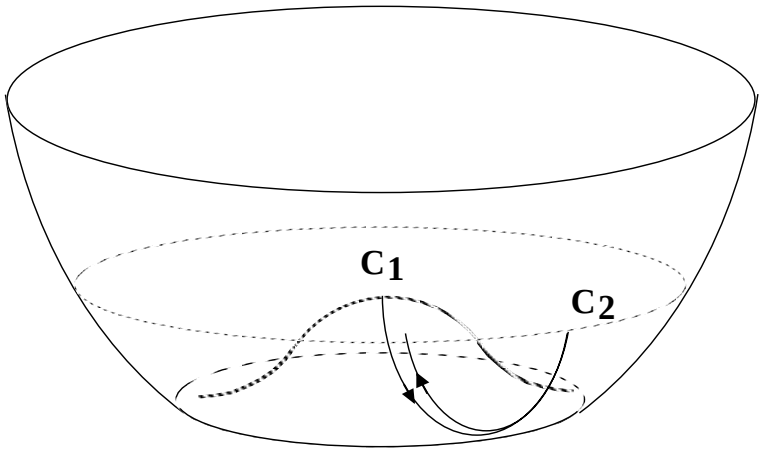

Fig. 23. In the inverted potential, the energy barrier becomes a well. In order to find the optimum trajectory which minimizes the action, one has to find a "bounce trajectory",[61] *i.e.* a trajectory which starts from C_1, goes down in the well, bounces at C_2 and comes back exactly at C_1 with zero velocity.

places V by -V. Then the system has a real evolution in a potential well. If one finds a particular trajectory which is such that the system goes from C_1 to C_2 and bounces back exactly to C_1, then this is the trajectory which optimizes the quantum action (Fig. 23).

Maris[37] first made a guess of what a good final configuration C_2 could be. For this he used a combination of cosine and gaussian functions. Then he used the equations of hydrodynamics in the inverted potential to calculate the real evolution of the system. He also neglected dissipation completely, which is certainly justified in the case of superfluid ^{4}He. He then optimized this configuration so that it bounces back on itself. He could also calculate the action and, in fact his numerical procedure converged more rapidly if he minimized both the action and the error in the bounce together. Once he had found an optimal trajectory at a given pressure, he repeated the calculation at all the successive pressures of interest and obtained $B(P)$. This calculation was done at $T = 0$, for ^{4}He and for ^{3}He.

At this stage, one might object that for the optimal trajectory, since the system reaches the final configuration with zero kinetic energy, it should take an infinite time. This is true except that the system always has fluctuations, either thermal or quantum, so that the condition of zero kinetic energy is only an approximation. In fact, the tunneling time is finite. Maris also noticed that, in a multidimensional space of configurations, the system does not necessarily go through the configuration which corresponds to the minimum energy barrier (a saddle point in the landscape).

As shown in Fig. 24, Maris found configurations which are about 10 Å in size and evolve in a "tunneling time" τ_t of order 20 to 40 ps. This time was about the ratio of the action B to the energy barrier E, as expected. He also found that, when starting close enough to the spinodal pressure, the critical nucleus was not empty, it was a broad shallow minimum in density, very different from the standard theory bubble. This is because the compressibility being large, it does not cost much energy to have density gradients extending over a large space. He then estimated, as usual, that, in the prefactor, the attempt frequency was the inverse of the tunneling time and that the density of independent sites was the inverse volume of the nucleus $[1/(10\text{Å})^3]$. He finally obtained a prediction for the tunneling rate and could compare it with the classical nucleation rate, in order to determine at which temperature T^* they had a comparable amplitude. He summarized his results in the graphs shown in Fig. 25: the cavitation pressure depends logarithmically on the product $V\tau$ as before. With no dissipation, the crossover is sharp between a temperature independent quantum regime which he had calculated at T=0 only, and the classical regime. With $V\tau$ in the range 10^{-10} to 10^{-20} cm^{3}s, he found no significant variation of T^*, which he predicted to be about 240 mK in ^{4}He and 120 mK in ^{3}He.

The Barcelona group. made a different kind of calculation with similar results.[64] They used Leggett's "functional integral approach" and calculated the crossover temperature from the oscillation frequency ω_b in the inverted potential. As shown in Fig. 26, T^* depends on the pressure $P_{\rm cav}$ at which cavitation occurs. This pressure changes if one varies the product $V\tau$. For a very small system, cavitation occurs very close to the spinodal limit. On the contrary, for a very large system, it may occur at much larger pressure. Guilleumas *et al.*[64] showed that T^* tends to zero in these two limits and has a maximum value in between, which is comparable to Maris'result. This is interesting but, for realistic values like $10^{-25} < V\tau < 1$ cm^{3}s, $P_{\rm cav}$ is only 0.1 to 0.5 bar above the spinodal limit, so that the crossover always takes place near the maximum of T^*(P).

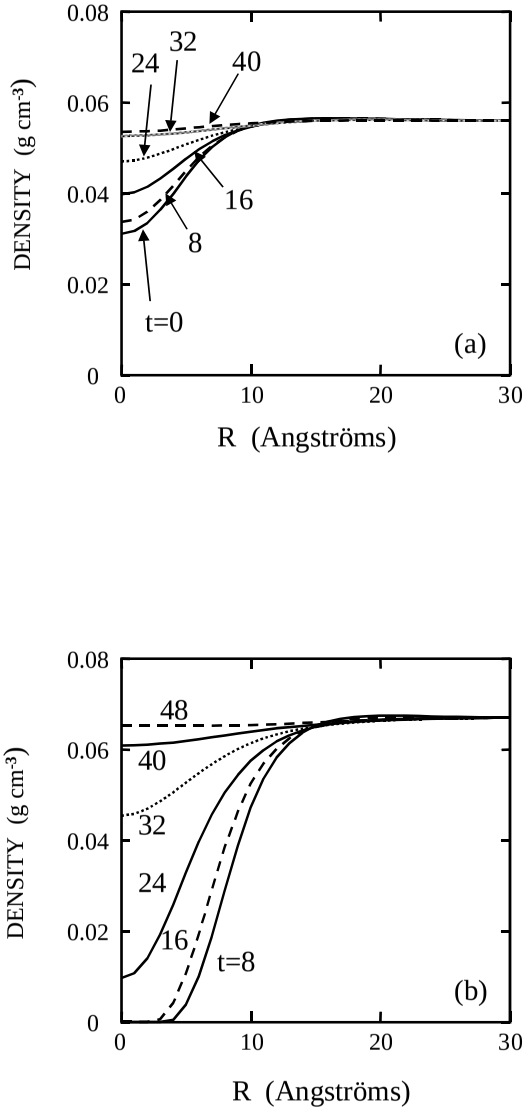

Fig. 24. Maris[37] calculated the optimal trajectory, *i.e.* the time evolution of the density field, both in ^{4}He and in helium 3. The two sets of curves reproduced here correspond to ^{3}He. In the upper graph labelled (a), the starting density is 0.056 g.cm^{-3}, *i.e.* very close to the spinodal limit and the density is non-zero at the center. When starting further away from the spinodal limit [0.067 g.cm^{-3}, graph (b)], the nucleus resembles more an empty bubble. Labels correspond to times in picoseconds.

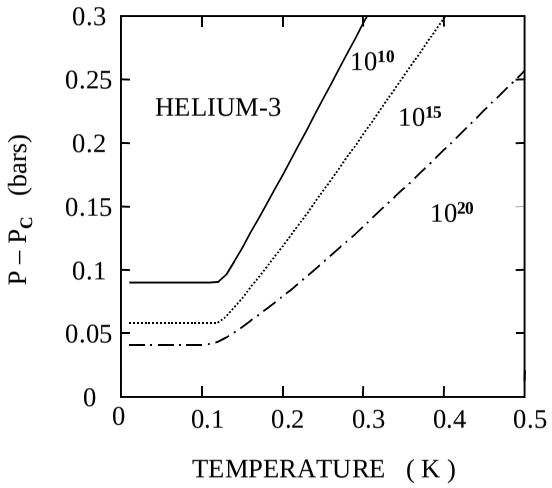

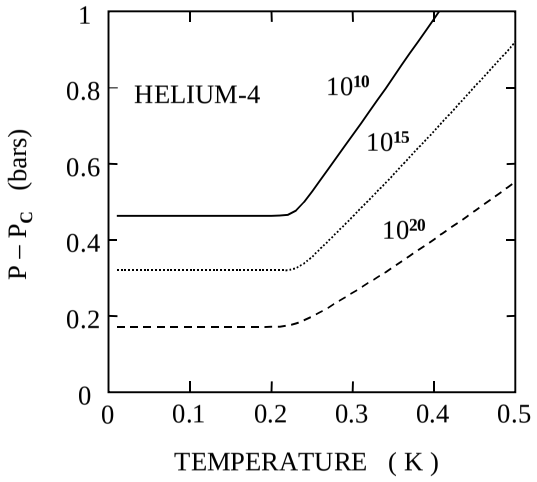

Fig. 25. As calculated by Maris,[37] the cavitation threshold shows a crossover from a quantum plateau at low temperature to a temperature dependent value in the thermally activated regime at higher temperature. Curves are drawn for different possible values of the product $V\tau$ of the experimental volume by the experimental time of the observation (more precisely $(V\tau)^{-1}$ in cgs units).

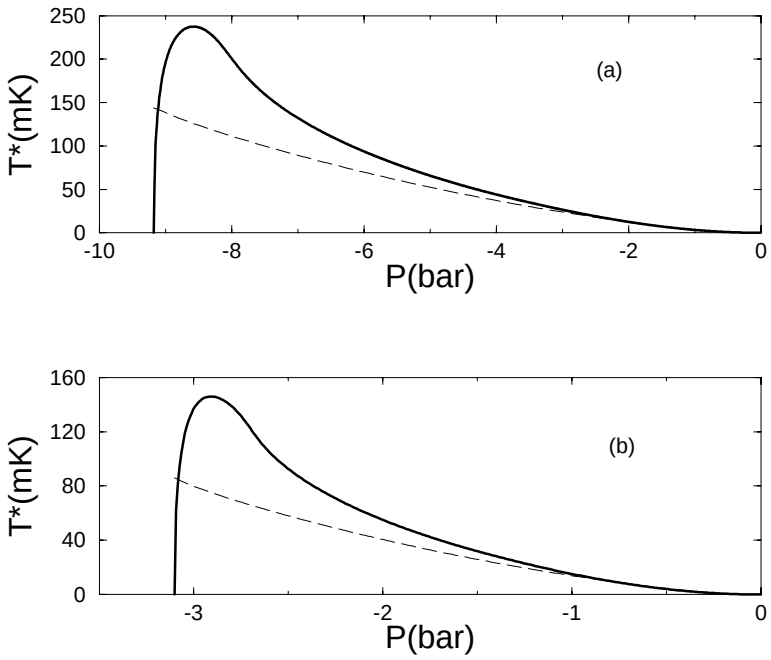

Fig. 26. The crossover temperature from quantum to classical nulcleation, as calculated by Guilleumas *et al.*[64] in both ^{4}He [top graph labelled (a)] and ^{3}He [lower graph labelled (b)]. In practice, experimental volumes and times are such that the crossover temperature is close to its maximum value. The broken line corresponds to the calculation in the thin wall approximation as done by Lifshitz and Kagan.[60]

4.3. Quantum Cavitation in Superfluid ^{4}He. Comparison with Experiments

Caupin *et al.*[23] have checked the common predictions of these two quantum theories in liquid helium. Their data show a rather large scatter in Fig. 13, but this is mostly due to the extrapolation used to calibrate the pressure. Since we are now more interested in temperature variations than in absolute pressures, it is better to come back to the raw data shown in Fig. 27. The three sets of measurements were done at three different static pressures in the cell. They all show a temperature independent plateau below 0.7 K, and a decrease of the cavitation threshold at higher temperature. In order to compare with theory, we used the following procedure. We knew that $V\tau$ was about 2.10^{-16} cm^{3}s in this experiment. Following Maris, we then estimated the prefactor as $\Gamma_0 = 1.7 \times 10^{31}$ cm^{-3}s^{-1} so that the action had to be $B = \ln(\Gamma_0 V\tau) = 35\ \hbar$ if the theory was correct. Furthermore, Maris

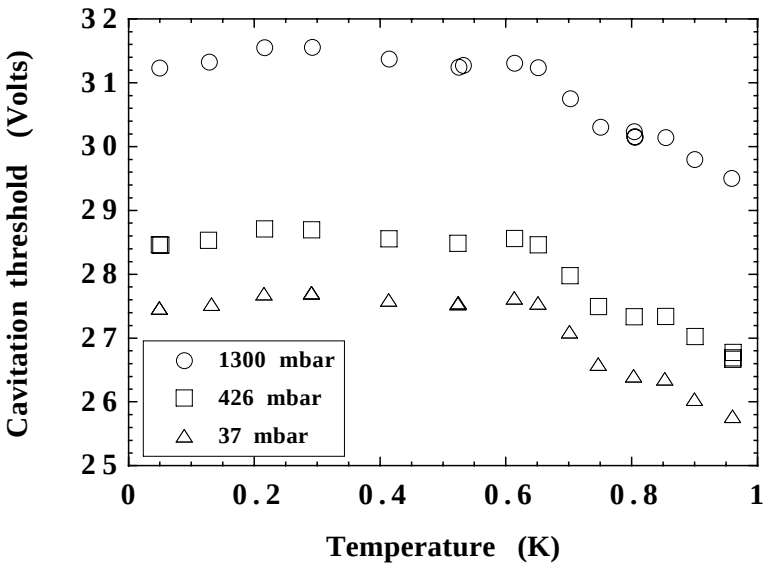

Fig. 27. As observed in ^{4}He by Caupin *et al.*,[23] the cavitation threshold shows the expected crossover from a quantum regime to a thermally activated one at higher temperature. The crossover temperature is found independent of the static pressure.

had calculated that the action B should be $35\hbar$ at $P = P_{\rm sp} + 0.25$ bar and according to the Barcelona group it had to be at $P_{\rm sp} + 0.34$ bar. These two values being inside the large error bars of the experimental measurements, we considered this first comparison as satisfactory. However, the theory also predicted a crossover temperature T^* three times lower than observed.

This was only an apparent contradiction. Indeed, 0.3 bar above the spinodal, the sound velocity c is strongly reduced compared to its value at positive pressure. According to the equation of state by Maris, it is 71 m/s at $P_{\rm sp} + 0.3$ bar, to be compared to 240 m/s at P = 0 bar. Since we used an acoustic wave to produce negative pressures, and since this wave was nearly adiabatic, there was a substantial temperature oscillation associated with the wave. The entropy of superfluid helium is proportional to $(T/c)^3$ in the low temperature region where phonons dominate the thermodynamics. As a consequence, when the pressure swing reached its minimum negative value, the temperature had to be reduced by the factor $240/71 = 3.4$ with respect to its static value. The temperature indicated in Fig. 27 is the static temperature in the cell of course, and it thus needs to be corrected by a fac-

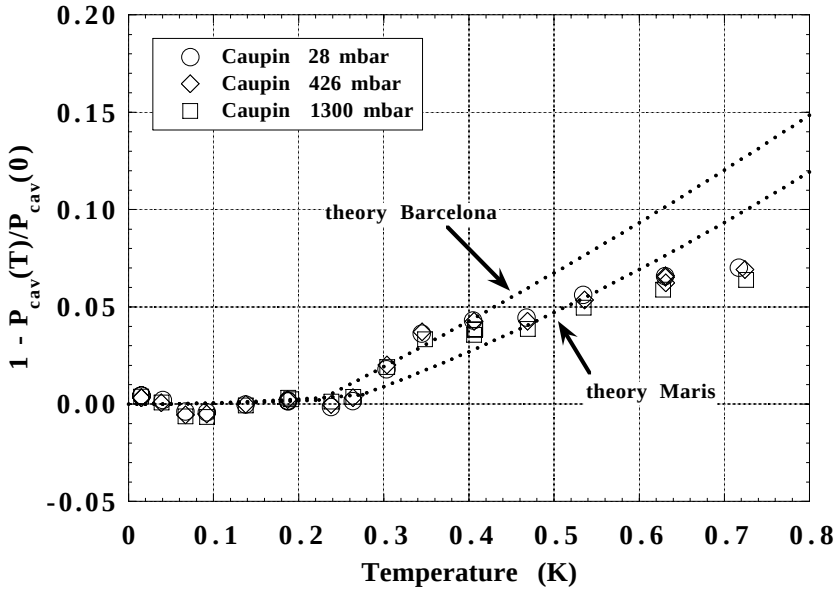

Fig. 28. Comparison of the temperature dependence of cavitation in ^{4}He with quantum cavitation theories. The experimental temperature has been corrected for the adiabatic cooling in the acoustic wave (see text).

tor 3.4 for the comparison with theory. We did a more precise temperature correction by using the recent calculation by Edwards and Maris of constant entropy curves in the phase diagram.[32] Once corrected this way, Caupin's results show a good agreement with the quantum nucleation theories (Fig. 28). The crossover temperature T^* is now correct and the temperature dependence of the classical regime has about the right magnitude as well. We have tried a last check with the width of the probability curve. In order to be precise, the measurement of this quantity needs an analysis of a very large number of events. As far as we can tell, the order of magnitude of this width is also consistent with theoretical predictions, but it would need further study, in particular the temperature dependence of this width in the classical regime should be studied carefully.

4.4. Nucleation in a Fermi Liquid: ^{3}He at Low Temperature

When studying liquid ^{3}He, Caupin *et al.*[23] found no crossover to a quantum cavitation regime at the temperature (120 mK) which had been pre-

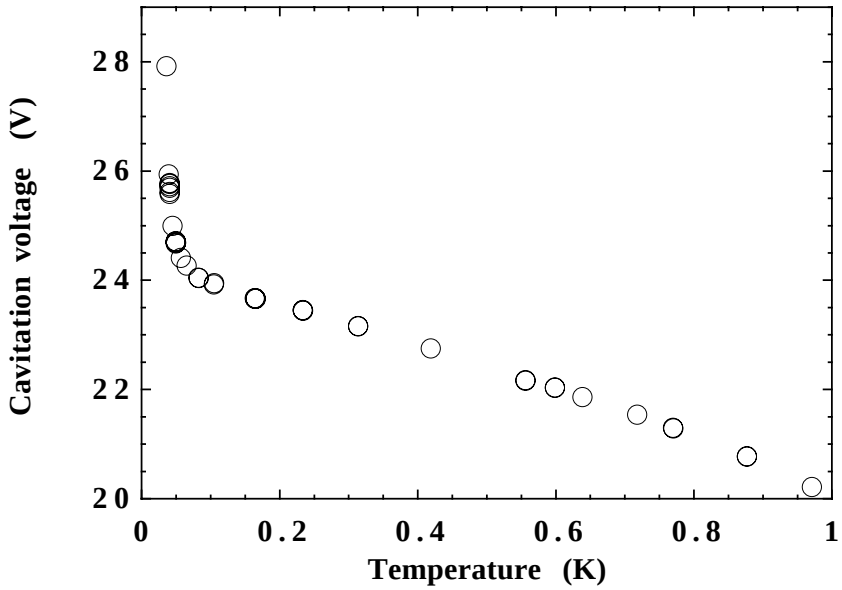

Fig. 29. The cavitation threshold voltage shows no quantum plateau in ^{3}He, as opposed to ^{4}He. This was attributed to the existence of a zero sound mode in Fermi liquids by Caupin et al.[46] (see text).

dicted. As shown in Fig. 29, instead of finding a plateau as in ^{4}He, Caupin *et al.* found a sudden increase of the cavitation threshold below 80 mK. Note, however, that the vertical coordinate on this graph is the voltage applied to the transducer, not the calibrated pressure at the acoustic focus.

At first sight, one could argue that this is because ^{3}He is not a superfluid. The quantum cavitation is a remarkable quantum tunnelling at a mesoscopic scale: liquid ^{4}He tunnels from a homogeneous density configuration to an inhomogeneous configuration which is some kind of hole concerning several hundreds of atoms. If the tunnelling resulted from the independent tunnelling of individual atoms, the tunnelling probability would include the product of a large number of small exponential factors and would be totally negligible. Is the superfluid coherence involved? Is it the macroscopic wave function of the superfluid liquid which extends through the barrier in configuration space and allows the system to tunnel? Yes, but what is needed is the coherence in a density wave, and this has nothing to do with the quantum coherence associated to superfluidity. In a solid at low temperature, there are quantum fluctuations of density, the zero point phonon modes, and no superfluidity. The coherence required for the tunnelling does not concern

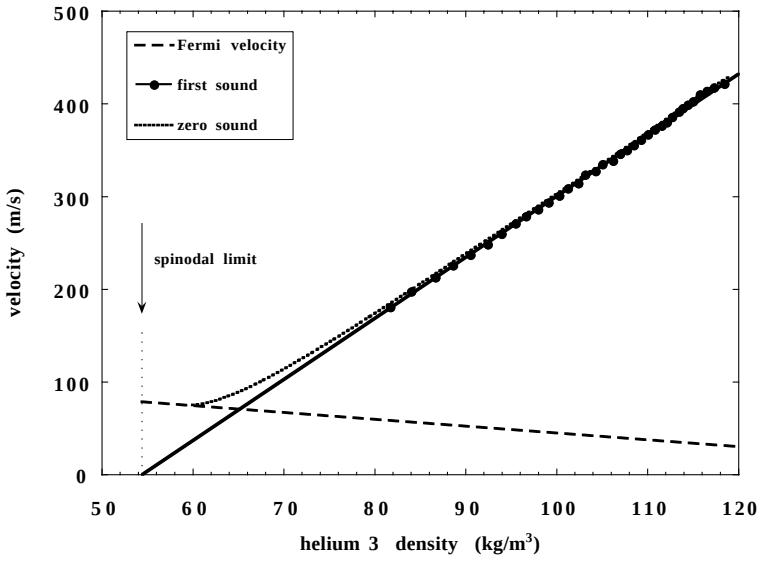

Fig. 30. The velocity of first sound tends to zero at the spinodal limit in liquid ^{3}He. On the contrary, the velocity of zero sound tends to the Fermi velocity which is finite.[66]

the same degrees of freedom as the superfluidity.

It has been argued also that liquid ^{3}He is a viscous liquid at low temperature, so that the quantum cavitation regime should be pushed down to much lower temperature than one initially thought.[65] This may be true, but it is the low frequency viscosity which diverges as $1/T^2$, and at the scale of our nucleus, dissipation seems much smaller. In fact, quasiparticles are ballistic on a scale of 10 Å at 100 mK, so that there seems to be no dissipation at all during the tunnelling time we have considered above. This leads us to another interpretation of Caupin's results which we think is more likely. It is a particular property of Fermi liquids.

At the spinodal limit, the diverging quantity is the static compressibility of the liquid. Only the low frequency sound has a vanishing velocity. Furthermore, being a Fermi liquid at low temperature, ^{3}He has a quantum stiffness at high frequency. As temperature decreases, the collision time between ^{3}He quasiparticles increases, and when it is larger than the sound period, the ordinary sound ("first sound") enters a collisionless regime called "zero sound". This quantum mode is a deformation of the Fermi surface which propagates in the liquid. At positive pressure in ^{3}He, the zero sound velocity c_0 is only slightly larger than the first sound velocity c_1. As pressure is reduced towards the spinodal limit, c_1 tends to zero but c_0 tends to the

Fermi velocity, which is about 80 m/s at -3 bar (Fig. 30).

In the above theory, the nucleation of bubbles proceeds via a density fluctuation with a short typical wavelength (10 Å). At 100 mK, sound waves with such wavelengths are well inside the zero sound ballistic regime, so that they are not soft, due to the presence of quantum effects which would need to be included in the theory. In fact, for the energy barrier to be low enough, one needs the radius R_c to be larger than the mean free path $l_{\rm qp}$ of quasiparticles, so that, nucleation proceeding in the hydrodynamic first sound mode, the energy barrier is small. The mean free path $l_{\rm qp}$ is 11 nm at 100 mK and 45 nm at 50 mK. The condition $R_c > l_{\rm qp}$ can be achieved because R_c diverges as P tends to the spinodal limit $P_{\rm sp}$. This divergence had been already noticed by Lifshitz and Kagan, and also found by Maris in his calculation. It is proportional to $(P - P_{\rm sp})^{-1/4}$, so that it happens only very close to $P_{\rm sp}$. For R_c to be 10 nm, one needs $P = P_{\rm sp} + 0.02$ mbar. Now, in such a vicinity of the spinodal limit, the non-linear effects become very large in the focusing of our acoustic wave: it is very difficult to build a negative pressure in a system which becomes infinitely soft. This is why cavitation suddenly needs a much larger voltage applied to the transducer. The temperature at which this happens is a crossover temperature from first sound to zero sound for density fluctuations of typically 1 to 10 nm wavelengths. It might still be possible to observe quantum cavitation in liquid ^{3}He, but, apparently, this should occur at a temperature much lower than originally thought.

5. CONCLUSION AND OPEN PROBLEMS

We have seen that the standard nucleation theory is simple and useful, and that it applies to many experimental situations where the radius of the critical nucleus is large enough. This was shown to be true with several examples. We have seen how many liquids can be studied in a metastable state, away from their equilibrium conditions. We then saw that at low temperature, nucleation may require that the system be under much larger departure from equilibrium so that the standard theory needs to be improved. The first of these improvements is the consideration of instabilities. A particularly important one is the spinodal limit, which is a bulk instability of the system whose response function diverge at a certain pressure which depends on temperature. It is best considered in the framework of density functional theories which proved very useful too. A further improvement is the consideration of quantum tunnelling, which is the only nucleation regime left when thermal fluctuations disappear. We have seen that the theory of

quantum nucleation is difficult in a system with many degrees of freedom such as a macroscopic sample of liquid at negative pressure. The theoretical understanding of this benefits a lot from the theory of the quantum escape out of a one-dimensional potential well. Results have been obtained in the case of the quantum cavitation in liquid ^{4}He. They support the available theoretical results, but the comparison is not yet as precise as was done for the tunneling of superconducting Josephson junctions.

To be exhaustive, I should have also considered cavitation in presence of electrons in liquid helium.[67] Electrons form bubbles which are well defined and well understood objects. In a sense, they are calibrated impurities which can be injected in liquid helium. Their study allowed other progresses, in particular a better understanding of how bubble chambers work.[68] I should also have considered cavitation in the presence of vortices. Maris[69] and Dalfovo[70] have shown that the presence of vortices lowers the cavitation threshold in superfluid ^{4}He, but no experiments have brought clear evidence for this mechanism yet.

If one considers the absence of nucleation as a possibility of studying metastable states, many interesting problems would need further investigation. Is the spinodal line of water monotonic in temperature or "re-entrant"? Is there a spinodal limit for the liquid/solid transition as well, and could it be observed by overpressurizing liquid helium very strongly? What is the exact shape of maximum density lines in water and in liquid helium in the metastable regions ? How does the superfluid transition (the "lambda line") extrapolate either at negative pressure or in highly overpressurized liquid ^{4}He? Would it be possible to study the influence of dissipation on quantum cavitation by adding ^{3}He impurities in superfluid ^{4}He? In fact, I have not considered the phase separation of mixtures either in these lectures, and it seems to me that there is not yet any consensus on the understanding of nucleation in ^{3}He/^{4}He mixtures.[71]

ACKNOWLEDGMENTS

I am very grateful to Harry Alles and the Low Temperature Laboratory at the Helsinki University of Technology for their invitation to give lectures at the Kevo Winter School. It has been a very stimulating opportunity for me to clarify what I presently understand and what, in my opinion, would need further work for a better understanding of nucleation in condensed matter. I am also grateful to H.J. Maris for a long permanent collaboration on this subject and to M. Barranco and M. Pi for sharing the latest numerical results of their calculations and many fruitful discussions during the past year.

REFERENCES

1. P. Taborek, *Phys. Rev. B* **32**, 5902 (1985).
2. Q. Zheng, D.J. Durben, G.H. Wolf and C.A. Angell, *Science* **254**, 829 (1991).
3. S. Balibar and H.J. Maris, *Physics Today* **53**, 29 (2000).
4. W.F. Pickard, *Prog. Biophys. Mol. Biol.* **37**, 181 (1981).
5. L. Landau and E. Lifshitz, *Statistical Physics*, Chapter 162, p. 533.
6. D.W. Oxtoby, *J. Phys.: Cond. Matt.* **4**, 7627 (1992).
7. M. Blander and J.L. Katz, *A.I.Ch.E. J.* **21**, 853 (1975).
8. H. Kramers, *Physica (Utrecht)* **7**, 284 (1940).
9. H. Grabert, P. Olshowski and U. Weiss, *Phys. Rev. B* **36**, 1931 (1987).
10. D.Turnbull and J.C. Fisher, *J. Chem. Phys.* **17**, 71 (1948).
11. M.S. Pettersen, S. Balibar and H.J. Maris, *Phys. Rev. B* **49**, 12062 (1994).
12. G. Seidel, H.J. Maris, F.I.B. Williams and J.G. Cardon, *Phys. Rev. Lett.* **56**, 2380 (1986).
13. H.J. Maris , G. Seidel and T.E. Huber, *J. Low Temp. Phys.* **51**, 471 (1983).
14. D.D. Osheroff and M. Cross, *Phys. Rev. Lett.* **38**, 905 (1977). See also Ref. 17.
15. A.J. Leggett, *Phys. Rev. Lett.* **53**, 1096 (1984).
16. S. Balibar, T. Mizusaki and Y. Sasaki, *J. Low Temp. Phys.* **120**, 293 (2000).
17. P. Schiffer, D.D. Osheroff and A.J. Leggett, *Prog. in Low Temp. Phys.*, Vol. XIV, ed. W.P. Halperin (Elsevier, 1995), p.159.
18. D. Bonn and D. Ross, *Rep. Prog. Phys.* **64**, 1085 (2001).
19. D.N. Sinha, J.C. Semura and L.C. Brodie, *Phys. Rev. A* **26**, 1048 (1982).
20. D. Lezak, L.C. Brodie, J.S. Semura and E. Bodegom, *Phys. Rev. B* **37**, 150 (1988).
21. J.A. Nissen, E. Bodegom, L.C. Brodie and J.S. Semura, *Phys. Rev. B* **40**, 6617 (1989).
22. H. Lambaré, P.Roche, S. Balibar, H.J. Maris, O.A. Andreeva, C. Guthmann, K.O. Kehsishev and E. Rolley, *Eur. Phys J. B* **2**, 381 (1998).
23. F.Caupin and S.Balibar, *Phys. Rev. B* **64**, 064507 (2001).
24. X. Chavanne, S. Balibar and F. Caupin, *J. Low Temp. Phys.* **125**, 155 (2001); X. Chavanne, S. Balibar and F. Caupin, *Phys. Rev. Lett.* **86**, 5506 (2001).
25. S. Balibar and P. Nozières, *Sol. State Comm.* **92**,19 (1994).
26. P. Nozières, in *Solids far from equilibrium, Lectures at the Beg-Rohu summer school*, ed. C. Godrèche (Cambridge University Press, 1992).
27. P.E. Wolf, F. Gallet, S. Balibar and P. Nozières, *J. Physique* **46**, 1987 (1985).
28. X. Chavanne, S. Balibar and F. Caupin, *J. Low Temp. Phys.* **126**, 615 (2002)
29. C. Appert, C.Tenaud, X. Chavanne, S. Balibar, F. Caupin and D. d'Humières, to be published; X. Chavanne, S. Balibar, F. Caupin, C. Appert and D. d'Humières, *J. Low Temp . Phys.* **126**, 643 (2002).
30. H.J. Maris and Q. Xiong, *Phys. Rev. Lett.* **63**, 1078 (1989).
31. H.J. Maris, *Phys. Rev. Lett.* **66**, 45 (1991).
32. D.O. Edwards and H.J. Maris, to be published.
33. J. Boronat, J. Casulleras and J. Navarro, *Phys. Rev. B* **50**, 3427 (1994).
34. F. Dalfovo, A. Lastri, L. Pricaupenko, S. Stringari and J. Treiner, *Phys. Rev. B* **52**, 1193 (1995).
35. J. Cahn and J. Hilliard, *J. Chem. Phys.* **31**, 688 (1959).

36. H.J. Maris *J. Low Temp. Phys.* **94**, 125 (1994).
37. H.J. Maris, *J. Low Temp. Phys.* **98**, 403 (1995).
38. A. Guirao, M. Centelles, M. Barranco, M. Pi, A. Polls and X. Vinãs, *J. Phys.: Cond. Mat.* **4**, 667 (1992).
39. For a general introduction to the physics of liquid helium, and a description of "rotons" which were introduced by Landau in 1941-47, see J. Wilks, *The properties of liquid and solid helium* (Clarendon Press, Oxford, 1967).
40. C.E. Campbell, R. Folk and E. Krotschek, *J. Low Temp. Phys.* **105**, 13 (1996).
41. G.H. Bauer, D.M. Ceperley and N. Goldenfeld, *Phys. Rev. B* **61**, 9055 (2000) and references therein.
42. S.C. Hall and H.J. Maris, *J. Low Temp. Phys.* **107**, 263 (1997).
43. M.Guilleumas, M.Pi, M. Barranco, J. Navarro, and M.A. Solis, *Phys. Rev. B* **47**, 9116 (1993).
44. M. Barranco and M. Pi, private communications (2002).
45. S.C. Hall, J. Classen, C.K. Su and H.J. Maris, *J. Low Temp. Phys.* **101**, 793 (1995).
46. F. Caupin, S. Balibar and H.J. Maris, *Phys. Rev. Lett.* **87**, 145302 (2001).
47. P.G. Debenedetti and M.C. d'Antonio, *J. Chem. Phys.* **84**, 3339 (1986) and *J. Chem. Phys.* **85**, 4005 (1986); M.C. d'Antonio and P.G. Debenedetti, *J. Chem. Phys.* **86**, 2229 (1987).
48. R.J. Speedy, *J. Phys. Chem.* **86**, 982 (1982) and *J. Phys. Chem.* **86** 3002 (1982).
49. S. Sastry, P.G. Debenedetti, F. Sciortino and H.E. Stanley, *Phys. Rev. E* **53**, 6144 (1996).
50. P.R. Roach, Y. Eckstein, M.W. Meisel and L. Aniola-Jedrzejek, *J. Low Temp. Phys.* **52**, 433 (1983).
51. C. Boghosian, H. Meyer and J.E. Rives, *Phys. Rev.* **146**, 110 (1966).
52. M.R. Gibbs, K.H. Andersen, W.G. Stirling, and H. Schober, *J. Phys.: Condens. Matter* **11**, 603 (1999).
53. M. Wanner and P. Leiderer, *Phys. Rev. Lett.* **42**, 315 (1979); W. Ebner and P. Leiderer, *Physics Letters* **80A**, 277 (1980).
54. T. Schneider and C.P. Enz, *Phys. Rev. Lett.* **27**, 1186 (1971).
55. J.P. Ruutu, P.J. Halonen, J.S. Pentila, A.V. Babkin, J.P. Saramäki and E.B. Sonin, *Phys. Rev. Lett.* **77**, 2514 (1996).
56. E.Varoquaux, M.W. Meisel and O. Avenel, *Phys. Rev. Lett.* **57**, 2291 (1986); J. Steinbauer, K. Schwab, Yu. Mukharski, J.C. Davis and R.E. Packard, *Phys. Rev. Lett.* **74**, 5056 (1995).
57. M.H. Devoret, J.M. Martinis and J. Clarke, *Phys. Rev. Lett.* **55**, 1908 (1985); J.M. Martinis, M.H. Devoret and J. Clarke, *Phys. Rev. Lett.* **55**, 1543 (1985).
58. L. Landau and E. Lifshitz, *Quantum Mechanics* (Pergamon, Oxford, 1965), Chapter 7.
59. J.S. Langer, *Ann. Phys.* **41**, 108 (1967)
60. I.M. Lifshitz and Yu. Kagan, *Sov. Phys. JETP* **62**, 385 (1972).
61. S. Coleman, *Phys. Rev. D* **15**, 2929 (1977), C.G. Callan and S. Coleman, *Phys. Rev. D* **16**, 1762 (1977)
62. A.O. Caldeira and A.J. Leggett, *Phys. Rev. Lett.* **46**, 211 (1981).
63. T. Nakamura, Y. Kanno and S.Takagi, *Phys. Rev. B* **51**, 8446 (1995).
64. M. Guilleumas, M. Barranco, D.M. Jezek, R.J. Lombard and M. Pi, *Phys. Rev.*

B **54**, 16135 (1996).
65. D. Jezek, M. Pi and M. Barranco, *Phys. Rev.* **B60**, 3048 (1999).
66. F. Caupin, S. Balibar and H.J. Maris, *J. Low Temp. Phys.* **126**, 91 (2001).
67. J. Classen, C.K. Su and H.J. Maris, *Phys. Rev. Lett.* **77**, 2006 (1996).
68. D. Konstantinov, W. Homsi, J. Luzuriaga, C.K. Su, M.A. Weilert and H.J. Maris, *J. Low Temp. Phys.* **113**, 485 (1998).
69. H.J. Maris, *J. Low Temp. Phys.* **94**, 125 (1994).
70. F. Dalfovo, *Phys. Rev. B* **46**, 5482 (1982).
71. For experiments, see V. Chagovets, I. Usherov-Marshak, G. Sheshin and A. Ya. Rudavskii, *J. Low Temp. Phys.* **110**, 473 (1998), E. Tanaka, K. Hatakeyama, S. Noma, S.N. Burmistrov and T. Satoh, *J. Low Temp. Phys.* **127** 81 (2002), and references therein; for theory, see D.M. Jezek, M. Pi, M. Barranco, R.J. Lombard and M. Guilleumas, *J. Low Temp. Phys.* **112**, 303 (1998), and M. Barranco, M. Guilleumas, M. Pi, D.M. Jezek and J. Navarro *Liquids under negative Pressure*, NATO Science Series, eds. A.R. Imre, H.J. Maris and P.R. Williams, (Kluwer, Dordrecht, 2002) as well as M. Barranco, M. Guilleumas, M. Pi and D. Jezek *Advances in quantum many-body theory*, eds. by E. Krotscheck and J. Navarro (World Scientific, London, 2002), Vol. 4, Chapter 7, and references therein.